

---

# **A Simulation Study of Turbofan Engine Deterioration Estimation Using Kalman Filtering Techniques**

---

Heather H. Lambert

---

June 1991



National Aeronautics and  
Space Administration

---

# A Simulation Study of Turbofan Engine Deterioration Estimation Using Kalman Filtering Techniques

---

Heather H. Lambert  
NASA Dryden Flight Research Facility, Edwards, California

1991



National Aeronautics and  
Space Administration

**Dryden Flight Research Facility**  
Edwards, California 93523-0273

# CONTENTS

<b>ABSTRACT</b>	<b>1</b>
<b>INTRODUCTION</b>	<b>1</b>
<b>NOMENCLATURE</b>	<b>2</b>
Symbols . . . . .	2
Greek . . . . .	3
Superscripts . . . . .	3
<b>ENGINE DESCRIPTION</b>	<b>3</b>
<b>MODEL DESCRIPTIONS</b>	<b>4</b>
<b>KALMAN FILTER DESIGN</b>	<b>5</b>
Application . . . . .	5
Design Iterations . . . . .	6
<b>KALMAN FILTER EVALUATION RESULTS</b>	<b>14</b>
Estimation With No Turbine Deterioration . . . . .	15
Estimation With High-Pressure Turbine Deterioration . . . . .	19
Estimation of Low-Pressure Turbine Deterioration . . . . .	25
Estimation With High- and Low-Pressure Turbine Deterioration . . . . .	32
Evaluation Summary . . . . .	38
<b>CONCLUSIONS</b>	<b>38</b>
<b>APPENDIX–KALMAN FILTER THEORY</b>	<b>39</b>
<b>REFERENCES</b>	<b>41</b>
<b>TABLES</b>	
Table 1. Design cases for the final Kalman filter design . . . . .	8
Table 2. Test case matrix for the Kalman filter evaluation . . . . .	14

## LIST OF FIGURES

Figure 1. The F100 EMD engine . . . . .	4
Figure 2. Comparison of simulation and reconstructed measurements for case III.	
(a) The $TT_{4.5}$ time histories . . . . .	9
(b) The $N_2$ time histories . . . . .	10
Figure 3. Efficiency estimates.	
(a) Case I . . . . .	11
(b) Case II . . . . .	12
(c) Case III . . . . .	13
Figure 4. Efficiency estimates.	
(a) Case 1 . . . . .	15
(b) Case 2 . . . . .	16
Figure 5. Comparison of simulation and reconstructed measurements for case 1.	
(a) The $PT_4$ time histories . . . . .	17
(b) The $TT_{4.5}$ time histories . . . . .	18
Figure 6. Efficiency estimates.	
(a) Case 3 . . . . .	19
(b) Case 4 . . . . .	20
(c) Case 5 . . . . .	21
(d) Case 6 . . . . .	22
Figure 7. Comparison of simulation and reconstructed measurements for case 6.	
(a) The $TT_4$ time histories . . . . .	23
(b) The $N_2$ time histories . . . . .	24
Figure 8. Efficiency estimates.	
(a) Case 7 . . . . .	26
(b) Case 8 . . . . .	27
(c) Case 9 . . . . .	28
(d) Case 10 . . . . .	29
Figure 9. Comparison of simulation and reconstructed measurements for case 10.	
(a) The $TT_{4.5}$ time histories . . . . .	30
(b) The $N_2$ time histories . . . . .	31
Figure 10. Efficiency estimates.	
(a) Case 11 . . . . .	32
(b) Case 12 . . . . .	33

(c) Case 13 . . . . .	34
(d) Case 14 . . . . .	35
<b>Figure 11. Comparison of simulation and reconstructed measurements for case 14.</b>	
(a) The $TT_{2.5}$ time histories . . . . .	36
(b) The $WCFAN$ time histories . . . . .	37
<b>Figure A-1. Kalman filter implementation . . . . .</b>	<b>40</b>

## ABSTRACT

Current engine control technology is based on fixed control parameter schedules derived for a nominal production engine. Deterioration of the engine components may cause off-nominal engine operation. The result is an unnecessary loss of performance, because the fixed schedules are designed to accommodate a wide range of engine health. These fixed control schedules may not be optimal for a deteriorated engine. This problem may be solved by including a measure of deterioration in determining the control variables. These engine deterioration parameters usually cannot be measured directly but can be estimated.

This document presents a Kalman filter design for estimating two performance parameters that account for engine deterioration: high- and low-pressure turbine delta efficiencies. The delta efficiency parameters model variations of the high- and low-pressure turbine efficiencies from nominal values. The filter has a design condition of Mach 0.90, 30,000-ft altitude, and 47° power lever angle (PLA). It was evaluated using a nonlinear simulation of the F100 engine model derivative (EMD) engine, at the design Mach number and altitude over a PLA range of 43° to 55°.

This work found that known high-pressure turbine delta efficiencies of -2.5 percent and low-pressure turbine delta efficiencies of -1.0 percent can be estimated with an accuracy of  $\pm 0.25$  percent efficiency with a Kalman filter. If both the high- and low-pressure turbine are deteriorated, then delta efficiencies of -2.5 percent to both turbines can be estimated with the same accuracy.

## INTRODUCTION

Current engine control technology is based on fixed control parameter schedules. These schedules are derived for a nominal production engine, however, very few engines actually match a nominal engine. Manufacturing tolerances lead to variations from a nominal engine. Given two new production engines, one may have better than nominal performance while the other has less than nominal performance. Larger variations result from deterioration of the engine components caused by normal component wear. The deterioration may be sufficient to cause off-nominal engine operation. Thus, the fixed control schedules derived for a nominal engine result in reduced performance for a deteriorated engine. One way to prevent this is to include a measure of deterioration in determining the control variables.

Engine component performance or deterioration parameters can be used to tune a nominal engine model to match a specific engine. These performance or deterioration parameters generally take the form of correction terms that can be added to engine design parameters, such as the low- and high-pressure turbine efficiencies, or compressor and fan airflows. The engine deterioration parameters are not directly measurable, but can be estimated.

Although several estimation techniques are available, Kalman filter techniques are particularly well suited to this estimation problem. The low- and high-pressure turbine delta efficiencies are assumed to vary slowly with respect to time, and thus can be modeled as system biases. Reference 1 addressed the use of Kalman filter techniques to estimate unknown system biases. If the state vector of a linear engine model is augmented to include the bias, or in this case, performance parameters, a Kalman filter can be designed to estimate the values. Reference 2 addressed the estimation problem for the F100 engine model derivative (EMD) engine and proposed a Kalman filter to estimate engine performance variations during flight. Reference 2 estimates five performance parameters, and includes nonlinear calculations in the filter design.

This report comprehensively documents one possible approach to applying Kalman filter methodology to estimating engine deterioration parameters for a F100 EMD engine using simulated data. The study demonstrates the process, therefore, the number of deterioration parameters estimated is limited to two: high- and low-pressure turbine delta efficiencies. The delta efficiencies model variations of the high- and low-pressure turbine efficiencies from nominal. When other types of deterioration exist, the estimator must be modified to encompass those types. The estimation process can be expanded to the identification of many more efficiency parameters, limited

only by the observability of the problem. Observability, in turn, is closely related to the number of independent measurements available.

The design process is presented for a F100 EMD turbofan engine at a flight condition of Mach 0.90, 30,000-ft altitude, and with a nominal power lever angle (PLA) of 47°. The design is based on a three-state engine model and includes more instrumentation than is available on a flight research engine. The results are evaluated using a comprehensive nonlinear simulation of the F100 EMD engine.

## NOMENCLATURE

### Symbols

$A, B, C, D, L, M$	state variable model matrices
$AJ$	nozzle area, in <sup>2</sup>
$CIVV$	fan inlet guide vane angle, deg
$e$	state reconstruction error
$E\{\}$	expected value
$K$	observer or Kalman filter gain matrix
$N_1$	low-pressure turbine rotor speed, rpm
$N_2$	compressor high-pressure turbine rotor speed, rpm
$P$	solution to the matrix Riccati equation
$PLA$	power lever angle, deg
$PT_{2.5}$	compressor inlet total pressure, psia
$PT_4$	burner exit total pressure, psia
$PT_6$	afterburner inlet total pressure, psia
$Q_{xx}$	state covariance matrix
$Q_{yy}$	measurement noise covariance matrix
$RCVV$	compressor stator vane angle, deg
$TT_{2.5}$	compressor inlet total temperature, °R
$TT_3$	burner inlet total temperature, °R
$TT_4$	burner exit total temperature, °R
$TT_{4.5}$	fan turbine inlet total temperature, °R
$TT_6$	afterburner inlet total temperature, °R
$TMT$	composite turbine metal temperature, °R
$u$	control vector
$u_0$	control vector trim prediction
$w_1$	process noise
$w_2$	measurement noise
$WCFAN$	fan air flow, lb/sec
$WCHPC$	compressor air flow, lb/sec

$WF$	gas generator fuel flow, lb/hr
$x$	state vector
$x_0$	state vector trim value
$y$	measurement vector
$y_0$	measurement vector trim value

### Greek

$\delta u$	control vector perturbation
$\delta x$	state vector perturbation
$\delta y$	measurement vector perturbation
$\eta_H$	high-pressure turbine delta efficiency, percent
$\eta_L$	low-pressure turbine delta efficiency, percent
$\sigma_j$	standard deviation of the noise associated with the $j$ th parameter
$\zeta$	engine deterioration vector

### Superscripts

$\cdot$	derivative with respect to time
$\hat{\cdot}$	parameter estimate
$T$	transpose of a matrix or vector

## ENGINE DESCRIPTION

The engine simulation used represents the F100 EMD engine (fig. 1). It is a low-bypass ratio, twin-spool, afterburning turbofan derived from the F100-PW-100 engine (Pratt and Whitney, West Palm Beach, Florida). The engine is controlled using a digital electronic engine control (DEEC). The DEEC is a full-authority, engine-mounted, fuel-cooled digital electronic control system that performs the functions of the standard F100 engine hydromechanical, unified fuel control, and the supervisory digital electronic engine control. A more detailed description of the engine can be found in reference 3.

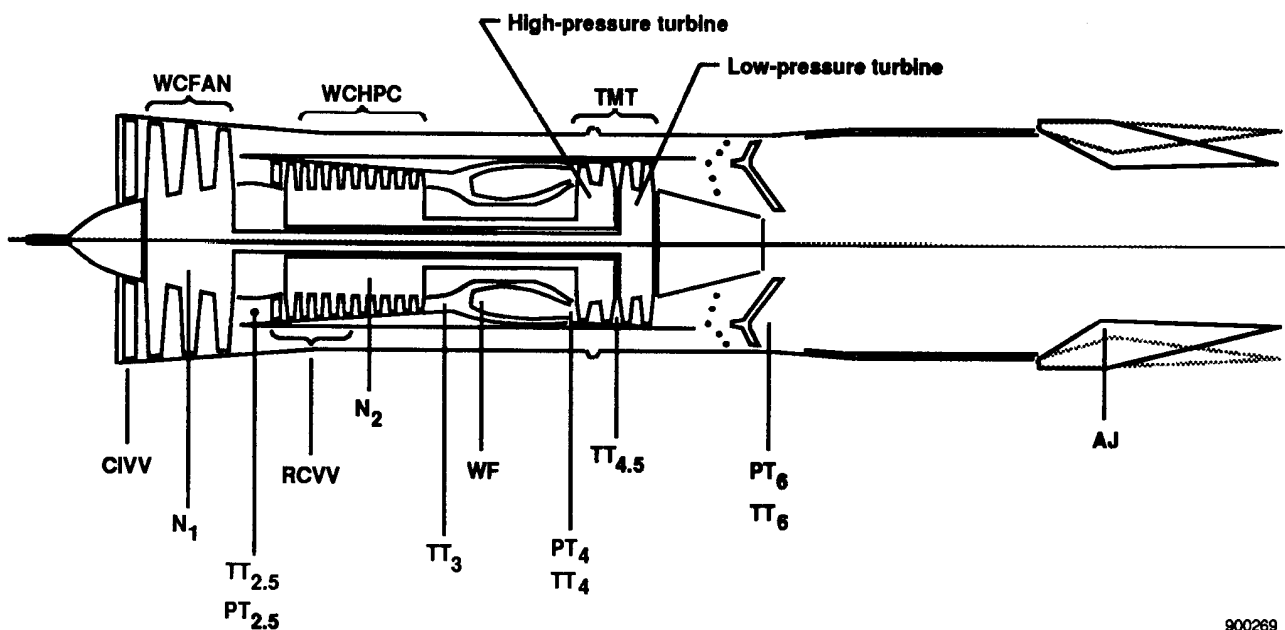
The following are the engine variables used in the Kalman filter design:

$CIVV$	fan inlet guide vane angle
$RCVV$	compressor stator vane angle
$N_1$	low-pressure turbine rotor speed
$N_2$	high-pressure turbine rotor speed
$PT_{2.5}$	compressor inlet total pressure
$TT_{2.5}$	compressor inlet total temperature
$TT_3$	burner inlet total temperature
$WCFAN$	fan airflow
$WCHPC$	compressor airflow
$WF$	gas generator fuel flow

$PT_4$	burner exit total pressure
$TT_4$	burner exit total temperature
$TT_{4.5}$	fan turbine inlet total temperature
$TMT$	composite turbine metal temperature
$PT_6$	afterburner total pressure
$TT_6$	afterburner total temperature
$AJ$	nozzle area

The deterioration parameters included in this study are:

$\eta_H$	high-pressure turbine delta efficiency
$\eta_L$	low-pressure turbine delta efficiency



900269

Figure 1. The F100 EMD engine.

## MODEL DESCRIPTIONS

Two engine models of an uninstalled F100 EMD engine are used in the Kalman filter design. One is a full-authority, nonlinear engine simulation provided by the engine manufacturer. It simulates engine operation throughout the entire engine operating envelope. This model is used to validate the filter design.

The second model is a state variable dynamic model (SVDM), also provided by the engine manufacturer. The SVDM is derived from the nonlinear simulation using perturbation methods. It is a piece-wise linear model containing 13 power points and simulates the full range of engine operation at the Mach 0.90, 30,000-ft altitude, and standard day flight condition. Each power point corresponds to a different PLA, and is comprised of dynamic matrices and trim values for the state, control, and measurement vectors. For this study, only one power point is examined; the power point selected has a trim PLA of  $47^\circ$ . The model point of  $47^\circ$  is expected to accommodate engine operation in the  $43^\circ$  to  $55^\circ$  trim PLA range. These represent the midpoints between the  $47^\circ$  model point and the two adjacent model points with trim PLAs of  $41^\circ$  and  $64^\circ$ , respectively. The study restricts engine operation to this range.

The original formulation of the SVDM is expressed as:

$$\delta \dot{x} = A\delta x + B\delta u \quad (1)$$

$$\delta y = C\delta x + D\delta u \quad (2)$$

where  $\delta x$ ,  $\delta y$ , and  $\delta u$  represent the perturbations of the state, measurement, and control vectors, respectively. The control and measurement perturbations,  $\delta u$  and  $\delta y$ , are calculated from the engine data:  $u$ ,  $y$ , and the control and measurement trim values ( $u_0$   $y_0$ ) where

$$\delta u = u - u_0 \quad (3)$$

and

$$\delta y = y - y_0 \quad (4)$$

The state vector includes the following variables:

$$x = \begin{bmatrix} N_1 \\ N_2 \\ TMT \end{bmatrix} \quad (5)$$

The control vector includes the following variables:

$$u = \begin{bmatrix} WF \\ AJ \\ CIVV \\ RCVV \end{bmatrix} \quad (6)$$

The measurement vector includes the following variables:

$$y = \begin{bmatrix} PT_6 \\ PT_{2.5} \\ PT_4 \\ TT_{2.5} \\ TT_3 \\ TT_4 \\ TT_{4.5} \\ TT_6 \\ WCFAN \\ WCHPC \\ N_1 \\ N_2 \\ TMT \end{bmatrix} \quad (7)$$

## KALMAN FILTER DESIGN

### Application

The original formulation of the linear engine model is given in equations (1) and (2). Deterioration can be added to the model as follows:

$$\delta \dot{x} = A\delta x + B\delta u + L\zeta + w_1 \quad (8)$$

$$\delta y = C\delta x + D\delta u + M\zeta + w_2 \quad (9)$$

where  $x$  is the state vector of dimension  $n$ ,  $u$  is the control vector of dimension  $r$ ,  $y$  is the measurement vector of dimension  $m$ ,  $\zeta$  is the vector of engine deterioration or performance parameters of dimension  $s$ , and  $w_1$  and  $w_2$  are the state excitation and measurement noise, which are white, uncorrelated, zero-mean, independent Gaussian processes with intensity  $Q_{xx}$  and  $Q_{yy}$ , respectively. The  $A, B, C, D, L$ , and  $M$  matrices are constant, with appropriate dimensions.

Engine deterioration generally occurs very slowly relative to the dynamics of the state variables. Thus,  $\dot{\zeta}$  can be approximated by 0. Engine deterioration can then be modeled as unknown bias terms. Reference 1 addressed the use of Kalman filters to estimate unknown system biases by augmenting the state vector to include the biases. The author's methodology can be applied to the estimation of engine performance parameters. If the state vector is augmented, assuming  $\dot{\zeta} = 0$ , then equations (8) and (9) can be rewritten as

$$\begin{bmatrix} \delta\dot{x} \\ \delta\dot{\zeta} \end{bmatrix} = \begin{bmatrix} A & L \\ 0 & 0 \end{bmatrix} \begin{bmatrix} \delta x \\ \delta\zeta \end{bmatrix} + \begin{bmatrix} B \\ 0 \end{bmatrix} [\delta u] + \begin{bmatrix} w_1 \\ 0 \end{bmatrix} \quad (10)$$

and

$$[\delta y] = \begin{bmatrix} C & M \end{bmatrix} \begin{bmatrix} \delta x \\ \delta\zeta \end{bmatrix} + \begin{bmatrix} D \end{bmatrix} [\delta u] + w_2 \quad (11)$$

This system representation can be used as the basis for the Kalman filter design.

The states, controls, measurements, and deterioration parameters were scaled for the filter implementation.

## Design Iterations

Once the linear model has been defined and scaled and the state and measurement covariances established, the Kalman filter design process is straightforward. The solution to the steady-state Riccati equation

$$\dot{P} = 0 = AP + PA^T + Q_{xx} - PC^T Q_{yy}^{-1} CP \quad (12)$$

is obtained (ref. 11), and the Kalman gain matrix is calculated from

$$K = PC^T Q_{yy}^{-1} \quad (13)$$

The variables in the design process are elements of the covariance matrices; the specific matrices selected can greatly affect the resulting Kalman gain matrix.

The measurement covariance matrix is the simpler of the two to determine. For this work, the simulated sensor noise is representative of noise found on flight data signals. The noise levels were approximated either from standard deviation data available from sensor manufacturers or were determined from flight data. The noise levels for the measured variables  $N_1, N_2, PT_4, PT_6$ , and  $TT_{4.5}$  were approximated from flight data and are consistent with those normally obtained from flight data. For each parameter, several time history segments of recorded flight data at Mach 0.90 and 30,000-ft altitude were analyzed for the mean values and the standard deviation ( $\sigma$ ). The largest standard deviation values were used to determine the covariance matrices. Most of the measurements are not commonly instrumented on actual engines. These are  $PT_{2.5}, TT_{2.5}, TT_3, TT_4, TT_6, WCFAN, WCHPC$ , and  $TMT$ . For these parameters, the ranges of values normally obtained are considered and theoretical noise levels estimated from sensors that measure similar ranges of values. The measurements tend to be clean, so the noise levels are at most

5 percent of the parameter ranges. The sensor noise estimates for the parameters are

$$\sigma_{w_2} = \begin{bmatrix} \sigma_{PT_6} \\ \sigma_{PT_{2.5}} \\ \sigma_{PT_4} \\ \sigma_{TT_{2.5}} \\ \sigma_{TT_3} \\ \sigma_{TT_4} \\ \sigma_{TT_{4.5}} \\ \sigma_{TT_6} \\ \sigma_{WCFAN} \\ \sigma_{WCHPC} \\ \sigma_{N_1} \\ \sigma_{N_2} \\ \sigma_{TMT} \end{bmatrix} = \begin{bmatrix} 0.09 \\ 0.1 \\ 0.6 \\ 1.0 \\ 2.5 \\ 7.0 \\ 5.0 \\ 3.75 \\ 0.5 \\ 0.1 \\ 15.0 \\ 15.0 \\ 7.0 \end{bmatrix} \quad (14)$$

and the associated measurement covariance matrix is

$$Q_{yy} = E\{w_2 w_2^T\} = \text{diag} \begin{bmatrix} \sigma_{PT_6}^2 \\ \sigma_{PT_{2.5}}^2 \\ \sigma_{PT_4}^2 \\ \sigma_{TT_{2.5}}^2 \\ \sigma_{TT_3}^2 \\ \sigma_{TT_4}^2 \\ \sigma_{TT_{4.5}}^2 \\ \sigma_{TT_6}^2 \\ \sigma_{WAT_2}^2 \\ \sigma_{WAT_{2.5}}^2 \\ \sigma_{N_1}^2 \\ \sigma_{N_2}^2 \\ \sigma_{TMT}^2 \end{bmatrix} \quad (15)$$

Once the measurement noise levels are established, the state excitation noise levels must be determined. In this case, the state excitation noise is unknown and is determined by trial and error through an iterative process. For each design iteration, a particular  $Q_{xx}$  is selected, and the Kalman gain matrix calculated. The filter is implemented and tested with various sets of data. One method of determining the performance of the filter is to compare the simulation measurements with the reconstructed measurements ( $y$  with  $\hat{y}$ ).

A preliminary design process was completed using time history data generated from the linear model given in equations (8) and (9). The data were generated using simultaneous step inputs to the four control variables, and with -1.0-percent deterioration to both the high- and low-pressure turbines. The purpose of the preliminary design process was to start converging on a value for  $Q_{xx}$ . This value was determined by an iterative process. The criterion for evaluating the performance of the preliminary design was the quality of the overplots of  $y$  and  $\hat{y}$ . The diagonal elements of  $Q_{xx}$  were modified to improve the filter performance by reducing the error between  $y$  and  $\hat{y}$ . The state covariance matrix was initially set to

$$Q_{xx} = \text{diag} \left[ 10^4 \quad 10^4 \quad 40.0 \quad 0.5 \quad 0.5 \right] \quad (16)$$

After numerous preliminary design iterations, a state covariance matrix of

$$Q_{xx} = \text{diag} \left[ \begin{array}{ccccc} 2450 & 900.0 & 93.75 & 0.0313 & 0.0313 \end{array} \right] \quad (17)$$

resulted in satisfactory performance.

A final design process was completed using data from a nonlinear engine simulation. Each design iteration was evaluated with three sets of data from this simulation. The data sets were time histories of the engine response for different levels of deterioration. In each case, steady-state engine operation was perturbed by the application of a PLA pulse. The PLA was held constant for 25 sec at 47° before a 25-sec pulse was applied. The pulse magnitudes varied for each case. Table 1 shows the pulse magnitudes and the delta efficiency levels used to generate each set of nonlinear simulation data. The three data sets cover the ranges of deterioration the filter should be able to estimate.

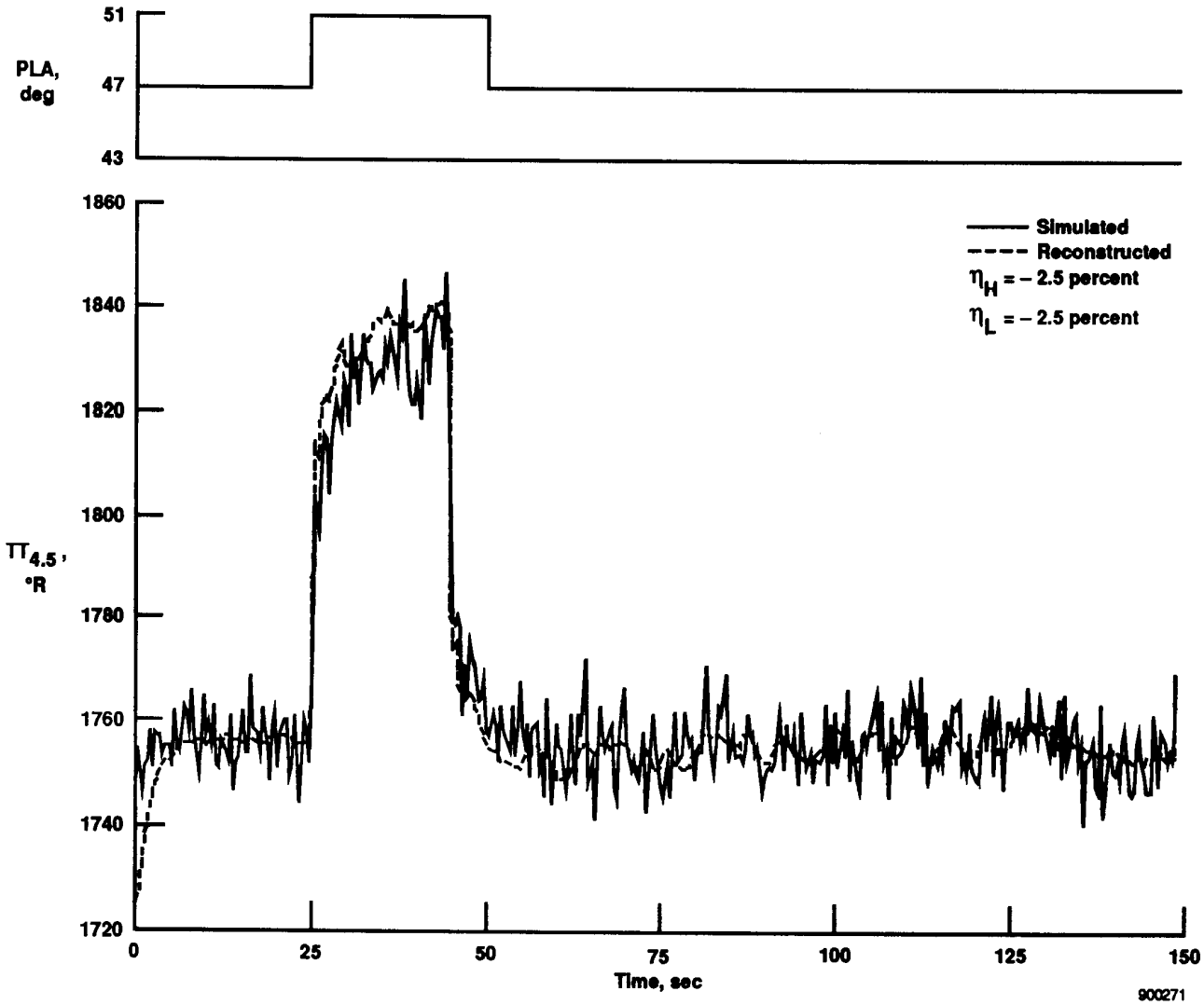
Table 1. Design cases for the final Kalman filter design.

Design case	Pulse magnitude, °PLA	High-pressure turbine delta efficiency, percent	Low-pressure turbine delta efficiency, percent
I	8	0.0	0.0
II	4	-1.0	-1.0
III	4	-2.5	-2.5

The application of a PLA pulse causes the engine operation to deviate from the trim conditions for the duration of the pulse. The off-trim operation is reflected primarily in the delta efficiency estimates, and appears as a pulse in the estimate time history. The estimates not only account for actual deterioration, but also for deviations from the efficiency trim condition.

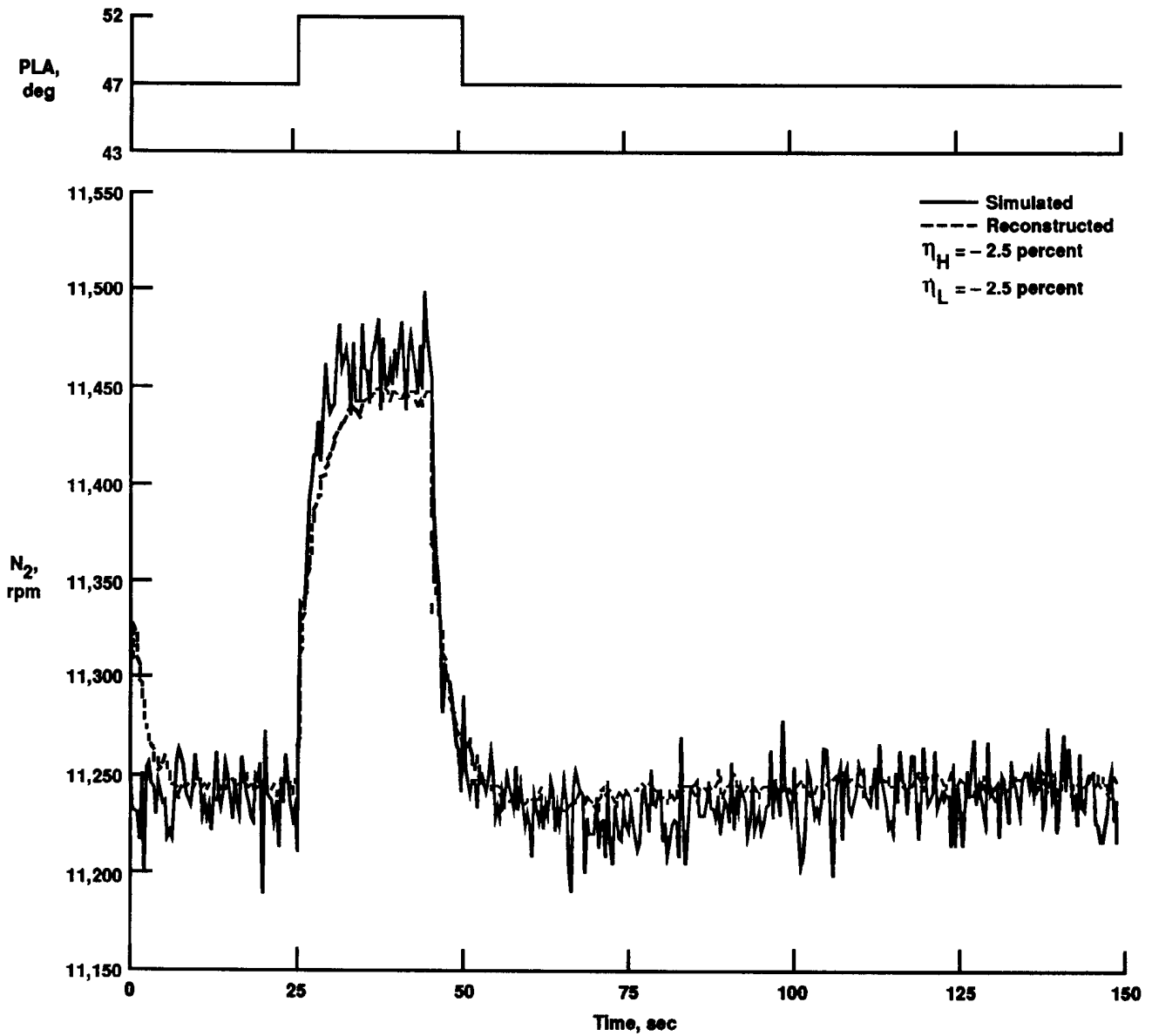
The final design was achieved with the following state excitation covariance matrix:

$$Q_{xx} = \text{diag} \left[ \begin{array}{ccccc} 857.5 & 720.0 & 31.25 & 0.0025 & 0.0031 \end{array} \right] \quad (18)$$



(a) The  $TT_{4.5}$  time histories.

Figure 2. Comparison of simulation and reconstructed measurements for case III.

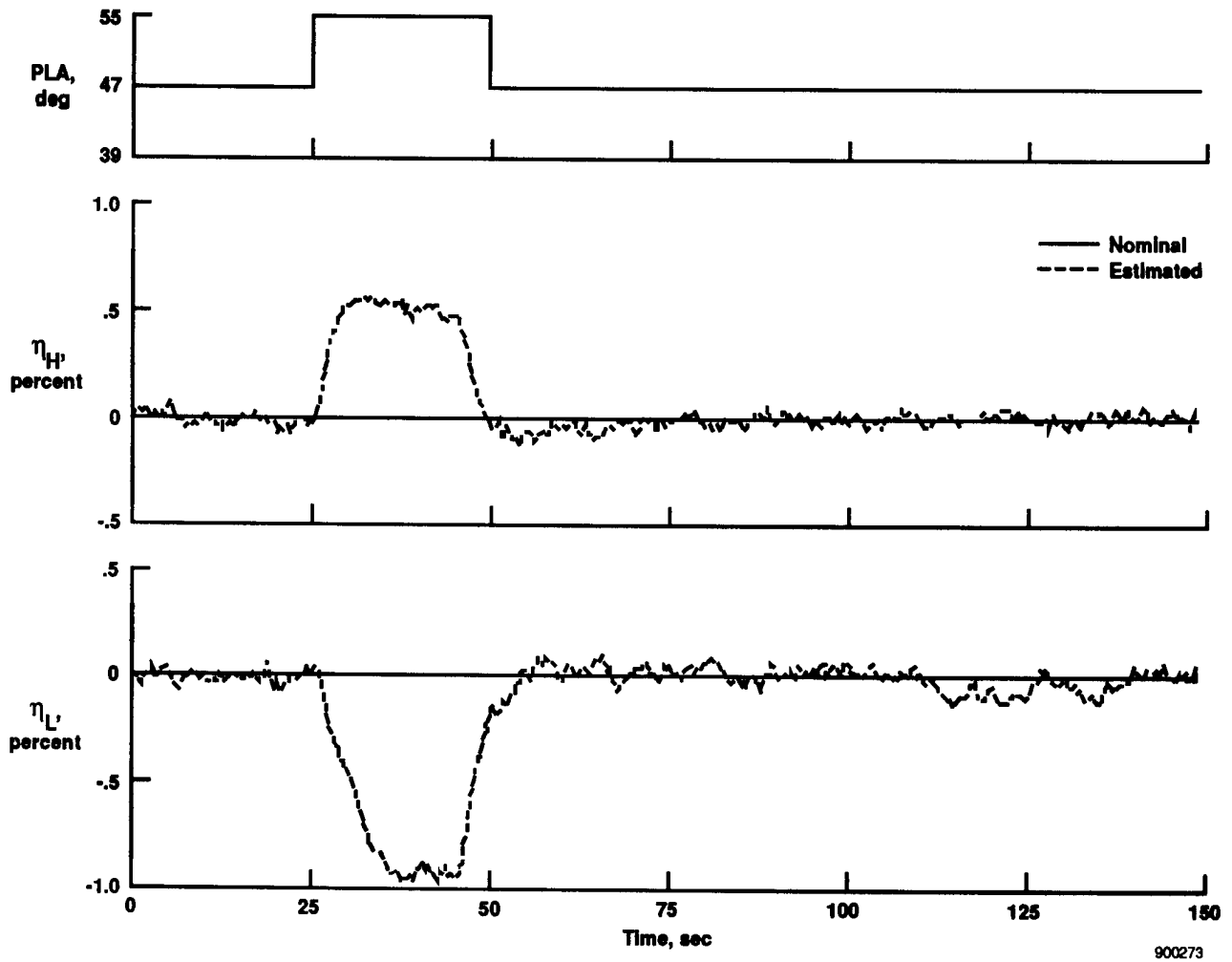


900272

(b) The  $N_2$  time histories.

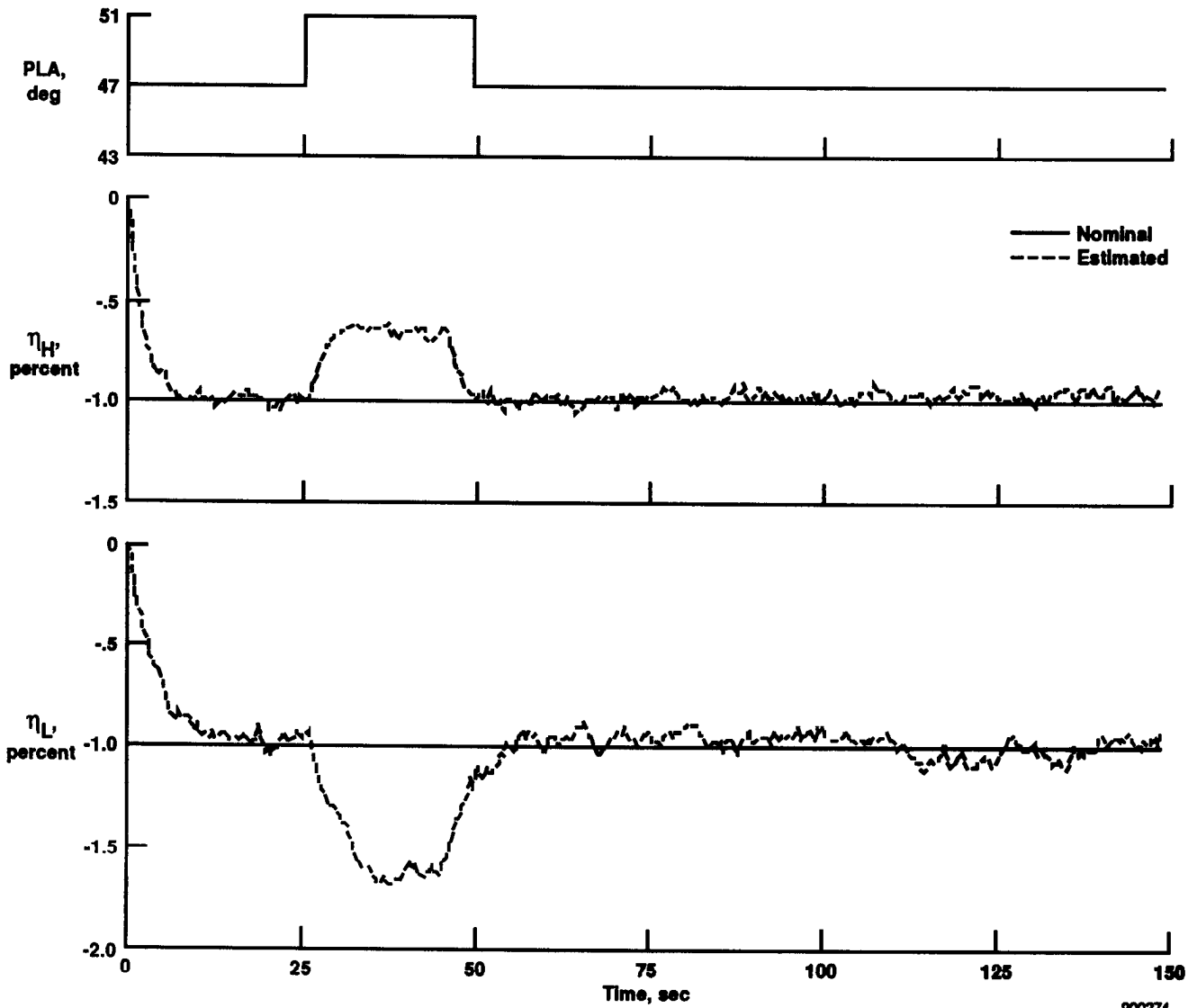
Figure 2. Concluded.

The results of the final design process are good. Figures 2(a) and (b) present time history overplots of the simulation and reconstructed measurements for the engine parameters  $TT_{4.5}$  and  $N_2$  and from case III. These are representative of the time history overplots achieved with the final design for all of the engine parameters in the three evaluation cases. Figures 3(a), (b), and (c) present time history comparisons of the delta efficiency levels input to the nonlinear simulation and the efficiency estimates for cases I, II, and III, respectively. The estimates for all three cases are within the desired accuracy of  $\pm 0.25$  percent of the nominal level.



(a) Case I.

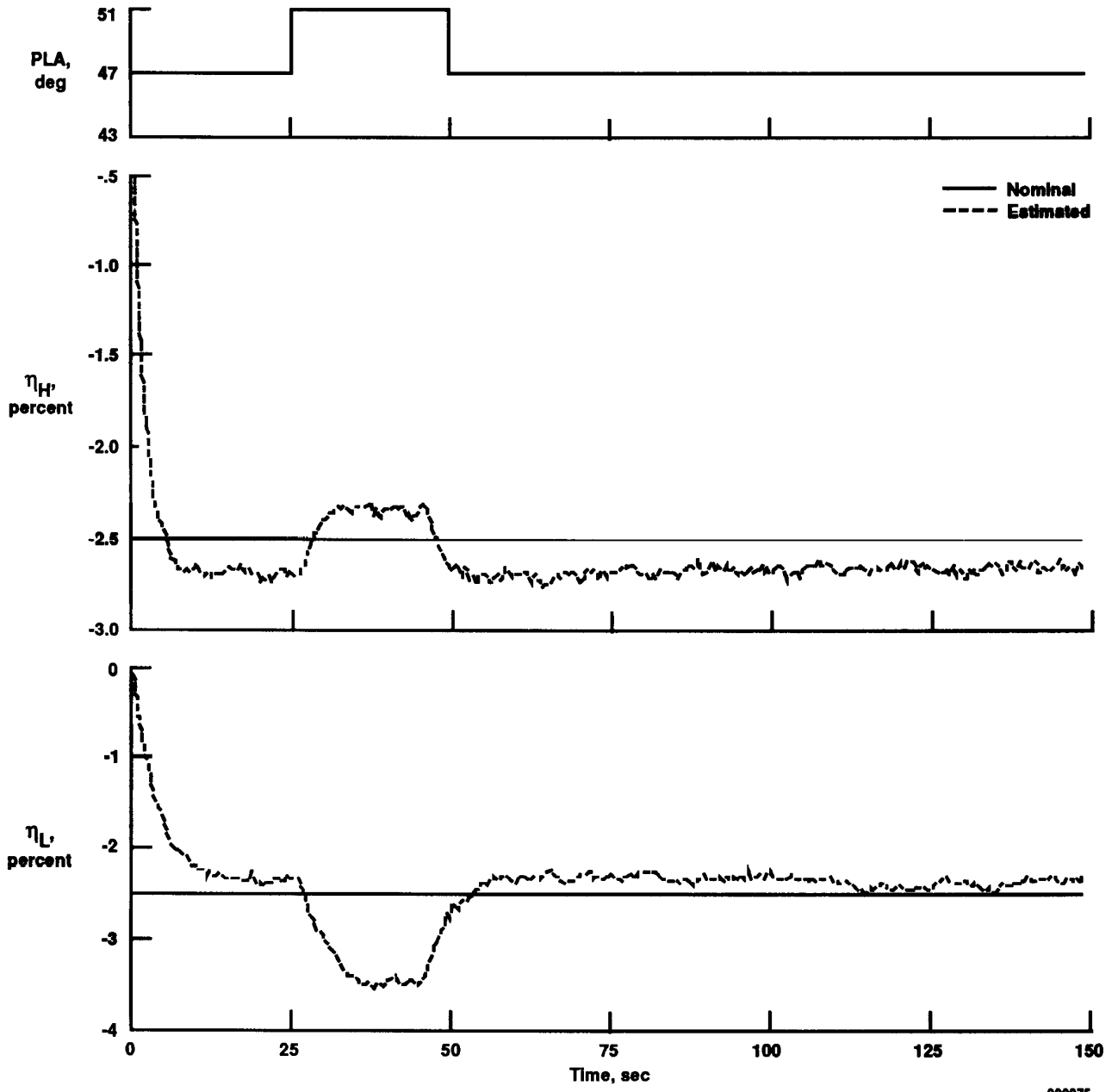
Figure 3. Efficiency estimates.



900274

(b) Case II.

Figure 3. Continued.



900275

(c) Case III.

Figure 3. Concluded.

The results for cases I and II are extremely good. In both cases the Kalman filter estimates of the high- and low-pressure turbine delta efficiencies differ from the nominal values by a few hundredths of 1-percent delta efficiency. The error is well within the desired accuracy of  $\pm 0.25$ -percent efficiency. The results for case III are also within the desired limits, but are poorer than the estimates for cases I and II. The estimate errors in case III are approximately 0.15-percent efficiency. The addition of  $-2.5$ -percent deterioration to the turbine efficiencies leads to unmodeled nonlinear effects, so the data begin to exceed the model linearity. In general, less accurate estimates occur with increased levels of deterioration, because of the nonlinear nature of engine degradation.

## KALMAN FILTER EVALUATION RESULTS

To evaluate the Kalman filter design more thoroughly, two types of test cases were obtained from the nonlinear engine simulation. The first type represents the engine response to a 25-sec PLA pulse about a steady-state condition. The pulse is applied after 25 sec of steady-state operation, and the level of deterioration is held constant throughout the time history. The cases differ in the steady-state PLA setting, the pulse magnitude, and the level of added deterioration. In the second type of test, the PLA is held constant throughout the entire time history, while the deterioration levels are modeled as step inputs to the system. The magnitude of the deterioration step inputs is  $-1.0$  percent, and they are applied to the nonlinear simulation after 20 sec. Table 2 shows a matrix of the test cases. For each test case, the initial steady-state PLA is assumed to be the trim PLA. If a PLA pulse is applied, the magnitude of the pulse is stated. The cases for which the delta efficiencies are modeled as step inputs are also noted.

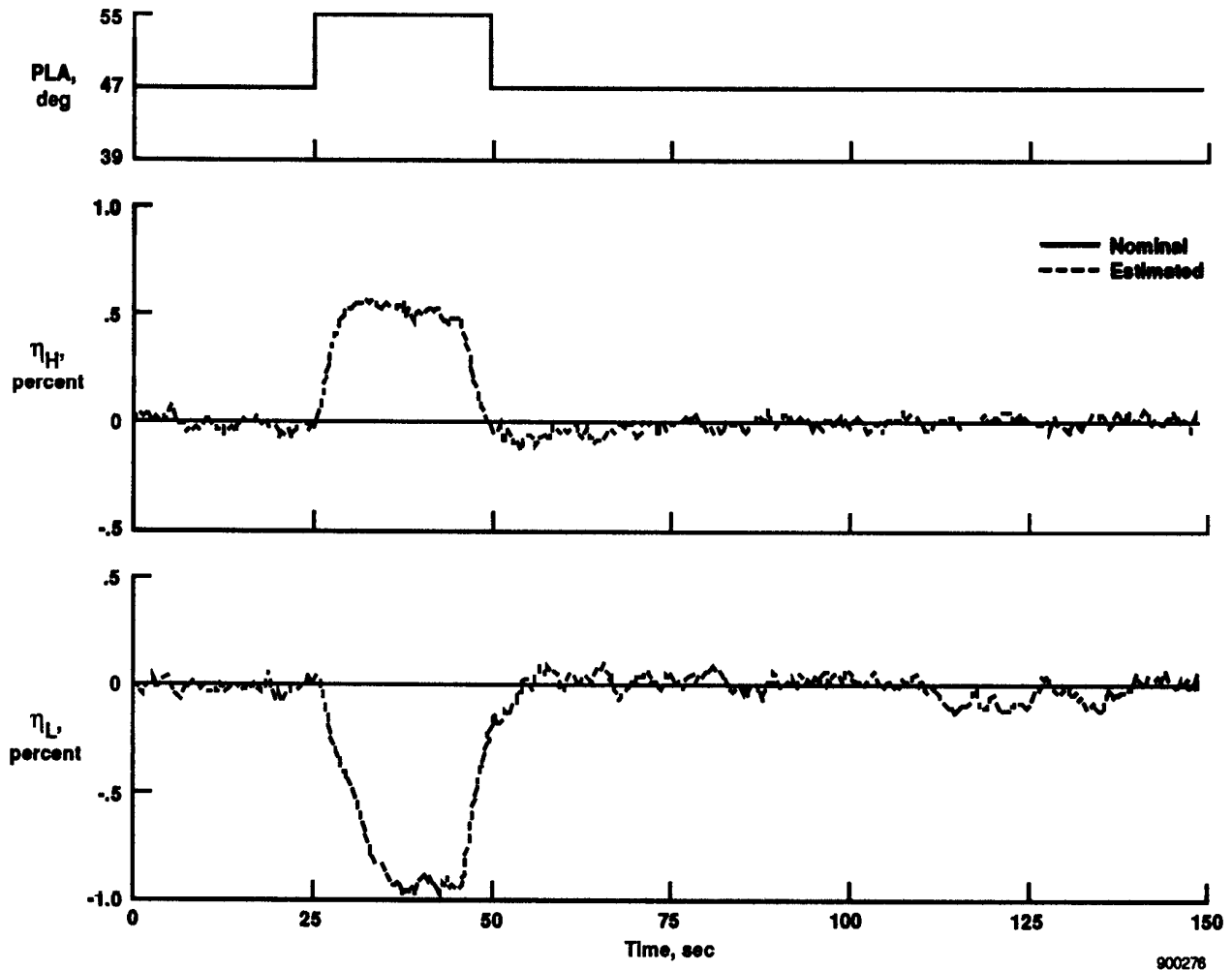
Table 2. Test case matrix for the Kalman filter evaluation.

Low-pressure turbine delta efficiency, percent	High-pressure turbine delta efficiency, percent			
	0.0	-0.5	-1.0	-2.5
0.0	Case 1, 47° PLA, 8° PLA pulse.	Case 3, 45° PLA, 4° PLA pulse.	Case 4, 47° PLA, 4° PLA pulse.	Case 6, 43° PLA, 4° PLA pulse.
	Case 2, 43° PLA, 8° PLA pulse.		Case 5, 45° PLA, step efficiencies.	
-0.5	Case 7, 51° PLA, -9° PLA pulse.	Case 11, 47° PLA, 4° PLA pulse.		
-1.0	Case 8, 47° PLA, 4° PLA pulse.		Case 12, 47° PLA, 4° PLA pulse.	
	Case 9, 45° PLA, step efficiencies.		Case 13, 45° PLA, step efficiencies.	
-2.5	Case 10, 55° PLA, -7° PLA pulse.			Case 14, 47° PLA, 4° PLA pulse.

The test cases can be organized into four categories: cases with no added deterioration, cases with added deterioration to the high-pressure turbine efficiency, cases with added deterioration to the low-pressure turbine efficiency, and cases with added deterioration to both turbine efficiencies. The evaluation results are discussed in four sections, each addressing one of the categories. To evaluate the quality of the estimates, the time histories of the efficiency estimates were compared to the nominal level input to the nonlinear simulation. The simulated and reconstructed measurements were also compared.

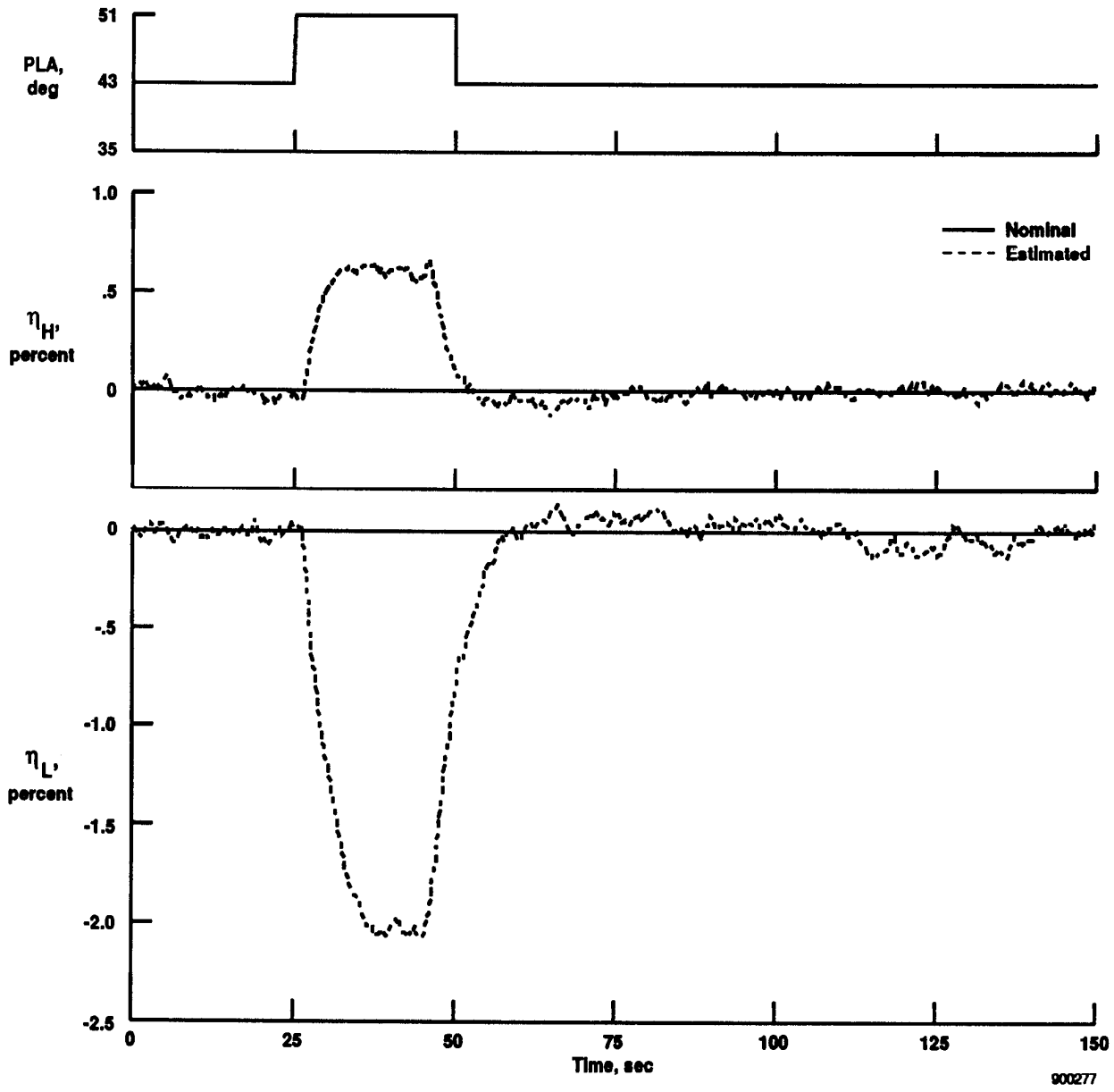
### Estimation With No Turbine Deterioration

Cases 1 and 2 represent engine operation with no added high- or low-pressure turbine deterioration. The efficiency estimates for case 1 are shown in figure 4(a), those for case 2 are shown in figure 4(b). For both cases the estimates are very good. The differences between the nominal and estimated delta efficiencies are of the same order of magnitude. Case 1 is generated at the model design PLA of  $47^\circ$ . The off-design steady-state PLA of  $43^\circ$  in case 2 does not further degrade the accuracy of the estimates relative to case 1. The measurement reconstructions for both cases are also very good. Figures 5(a) and (b) are representative of the time history comparison of the simulation and reconstructed measurements for an undeteriorated engine. Figure 5(a) is the time history overplot for  $PT_4$  for case 1. Figure 5(b) is the time history overplot for  $TT_{4.5}$  for case 2.



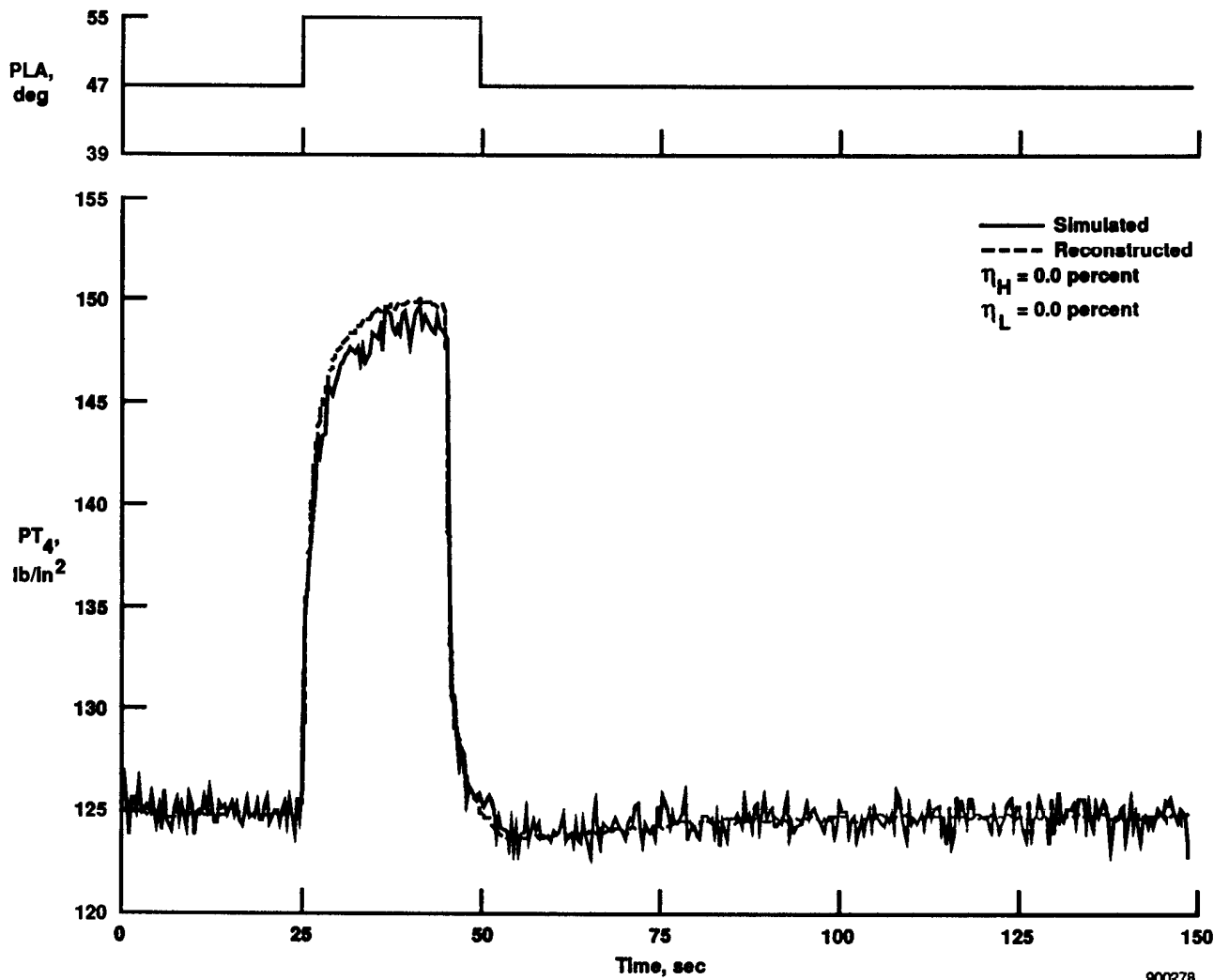
(a) Case 1.

Figure 4. Efficiency estimates.



(b) Case 2.

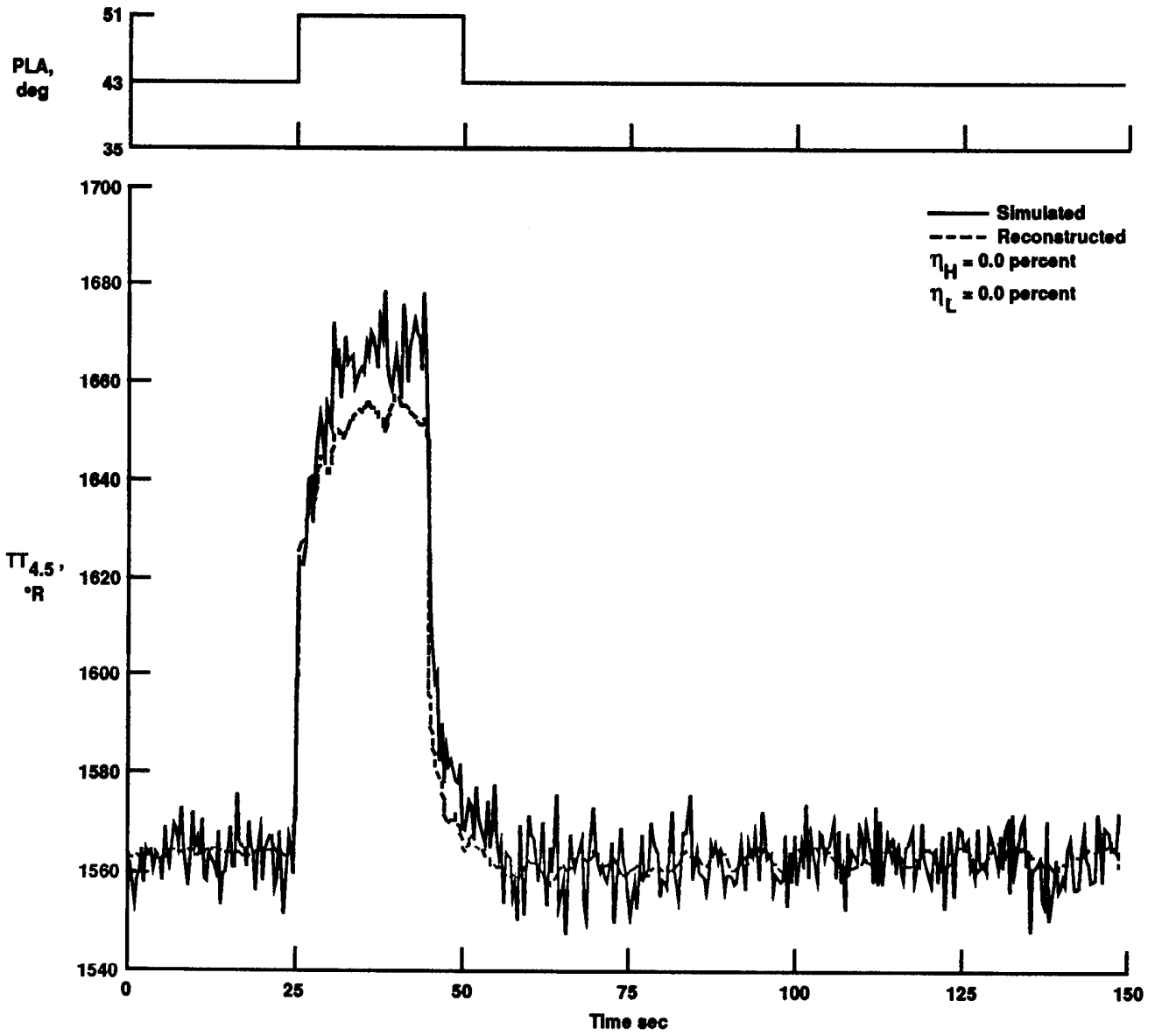
Figure 4. Concluded.



900278

(a) The  $PT_4$  time histories.

Figure 5. Comparison of simulation and reconstructed measurements for case 1.

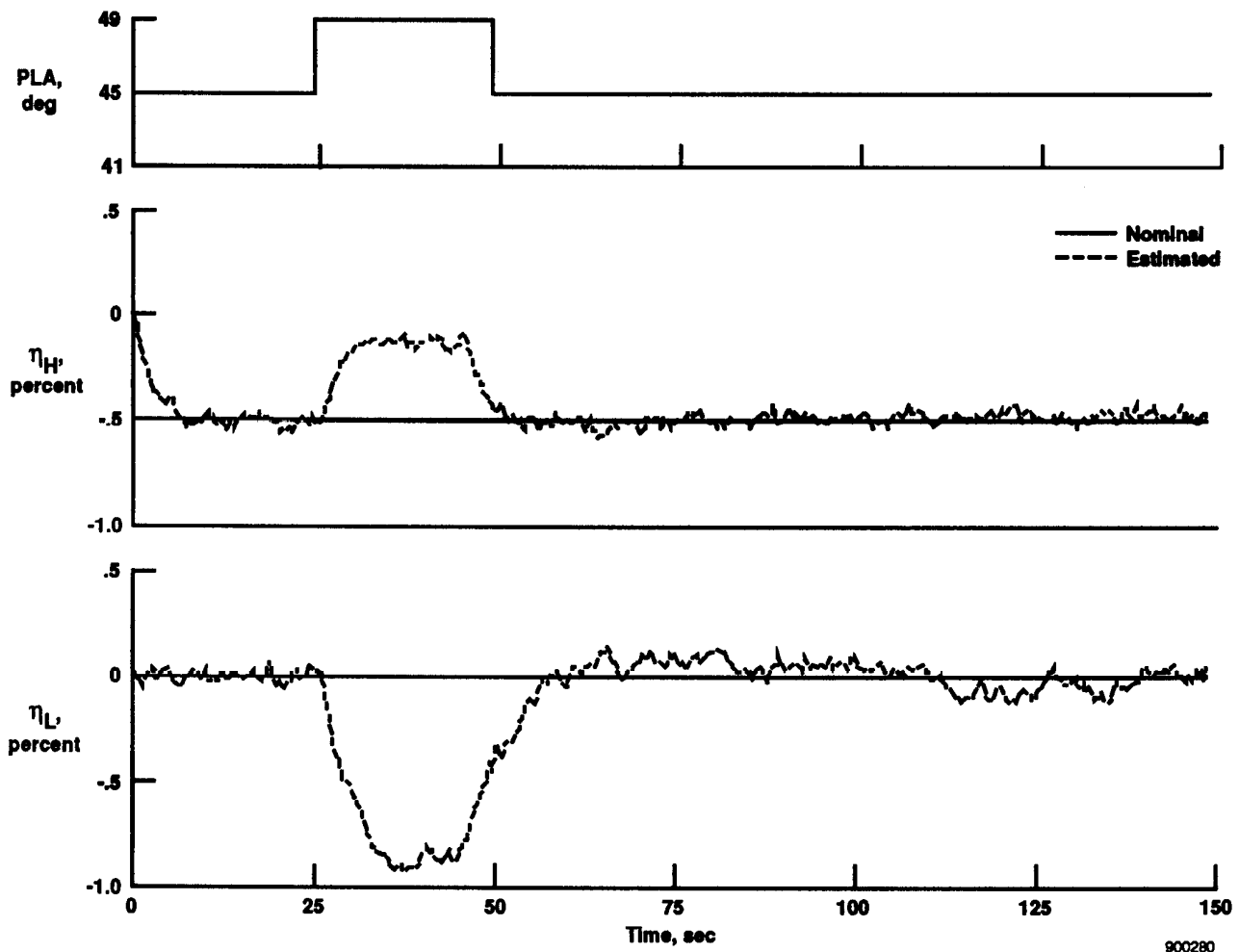


900279

(b) The  $TT_{4.5}$  time histories.  
 Figure 5. Concluded.

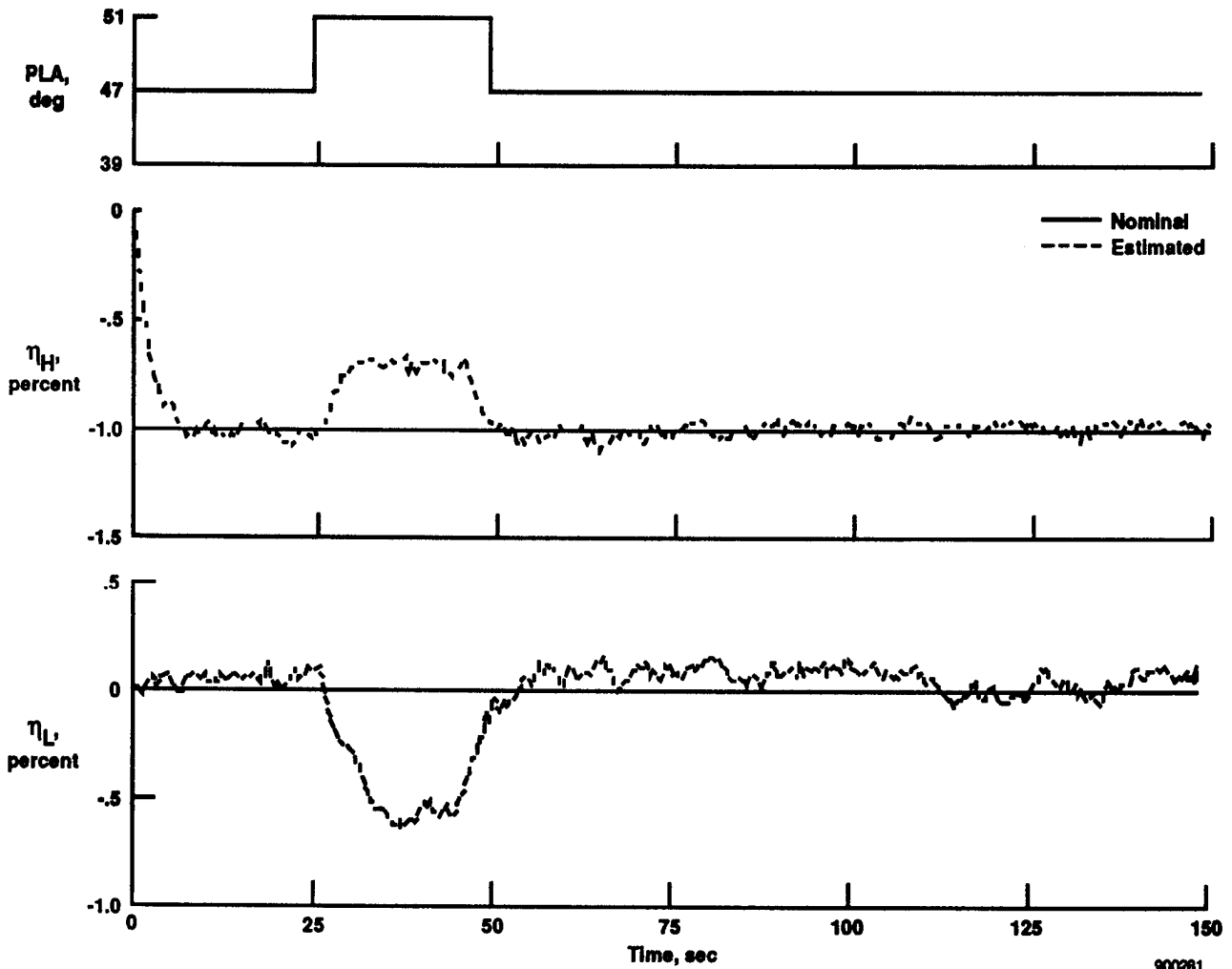
## Estimation With High-Pressure Turbine Deterioration

Cases 3, 4, 5, and 6 represent degraded high-pressure turbine efficiency. Figures 6(a)–(d) show the efficiency estimates for cases 3, 4, 5, and 6. The results for cases 3, 4, and 5 are very good. The filter can easily accommodate  $-1.0$ -percent added high-pressure turbine deterioration with the desired accuracy of  $\pm 0.25$  percent. The off-design steady-state operation in cases 3 and 5 does not degrade the accuracy of the efficiency estimates. The estimates for case 6, particularly  $\eta_L$ , are poorer than the other cases. The  $\eta_H$  estimate error of  $0.11$ -percent efficiency is still within the desired accuracy. The  $\eta_L$  estimate has an error of  $0.45$ -percent efficiency, which exceeds the desired accuracy. The addition of  $-2.5$ -percent high-pressure turbine delta efficiency causes nonlinear effects that exceed the linear range of the model, adversely affecting the filter estimates. The off-design steady-state  $43^\circ$  PLA in case 6 may further contribute to the  $\eta_L$  estimate degradation. The poor efficiency estimates for case 6 are reflected in the measurement reconstructions. Many of the measured parameters show noticeable differences between the simulation and reconstructed measurement values. These parameters are  $TT_3$ ,  $TT_4$ ,  $TT_{4.5}$ ,  $WCHPC$ , and  $N_2$ . Figures 7(a) and (b) present time history overplots of the simulation and reconstructed measurements for  $TT_4$  and  $N_2$  for case 6. These figures are representative of the parameters that reflect the poorer efficiency estimates in case 6.



(a) Case 3.

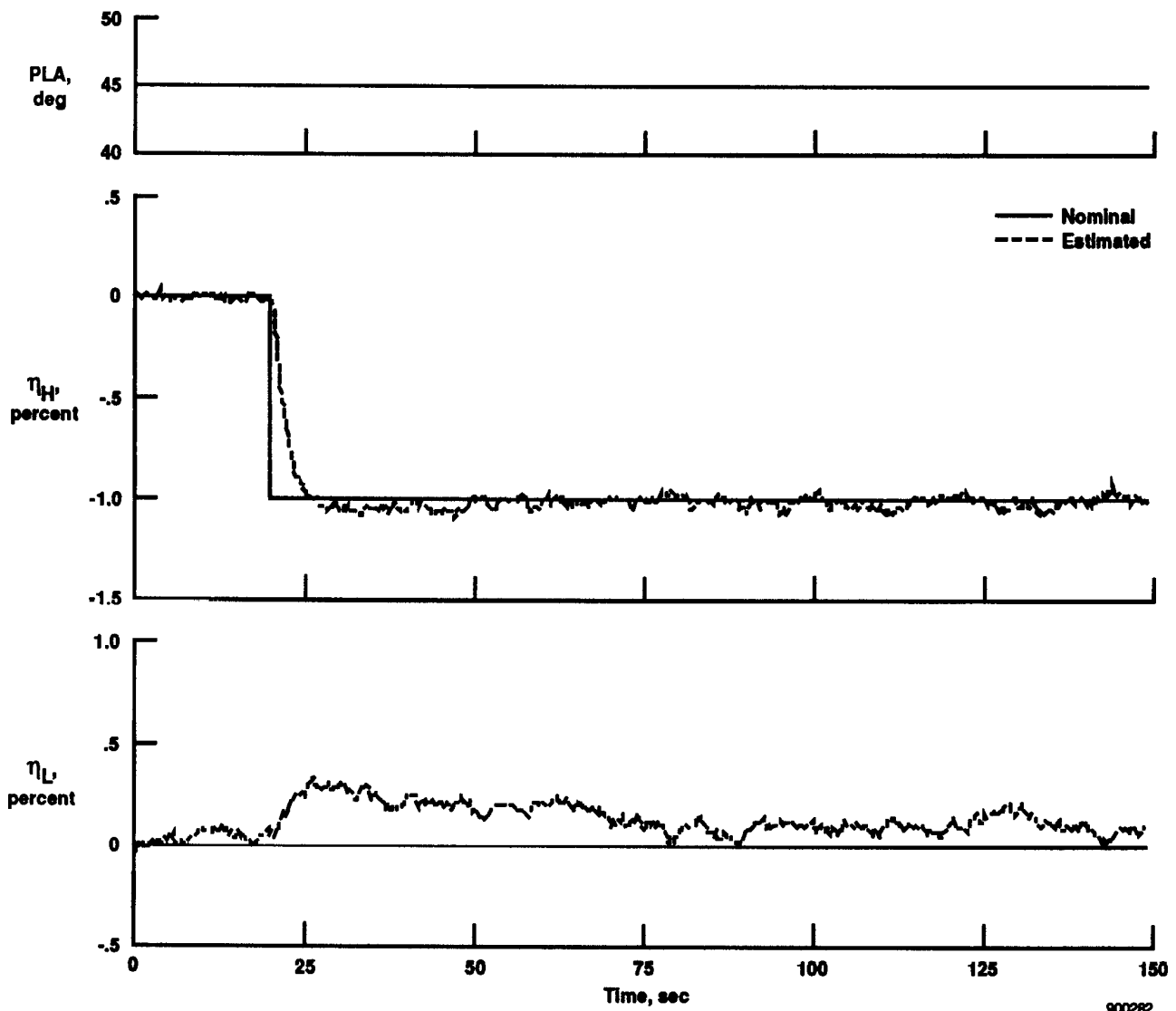
Figure 6. Efficiency estimates.



900281

(b) Case 4.

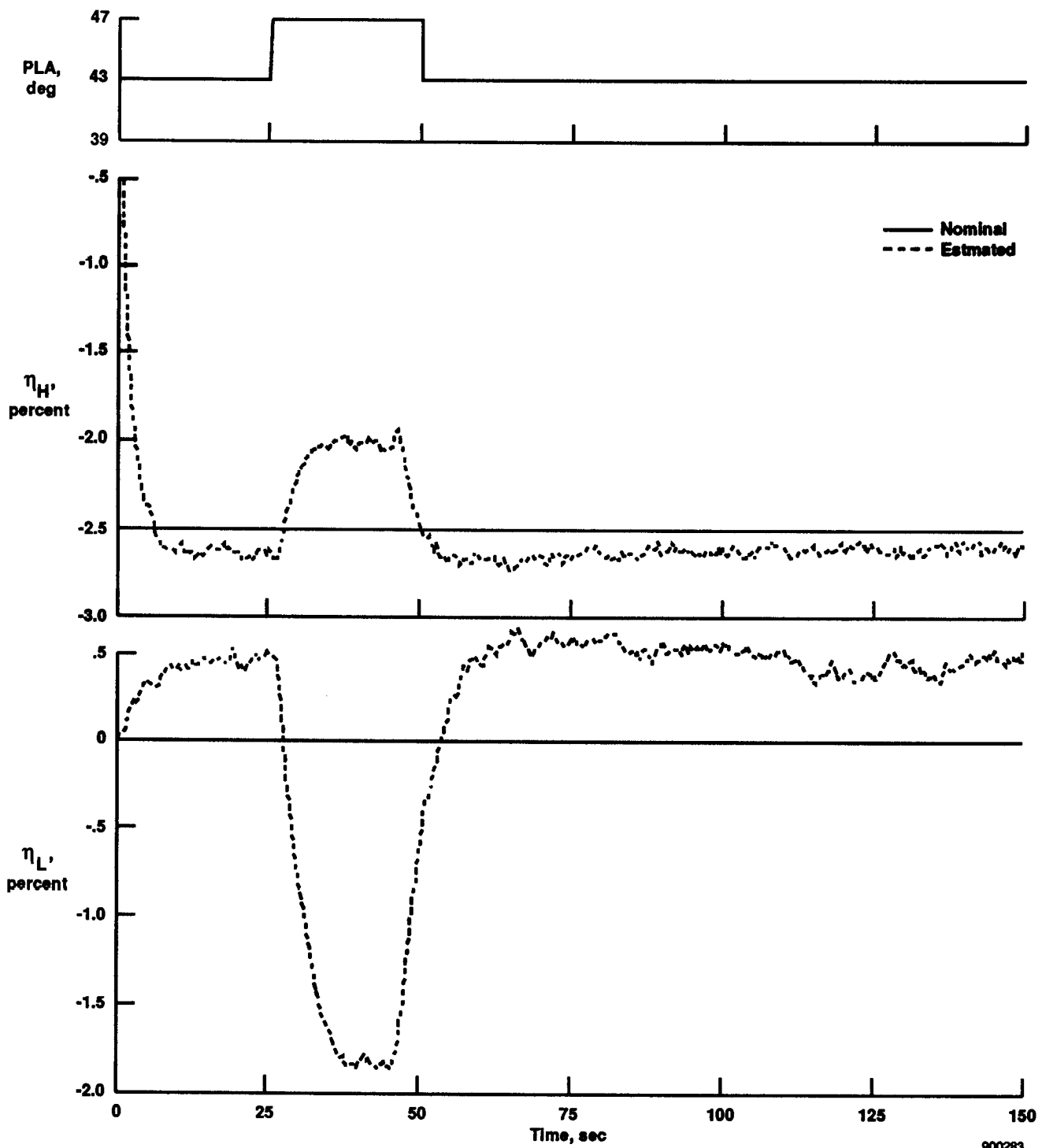
Figure 6. Continued.



900282

(c) Case 5.

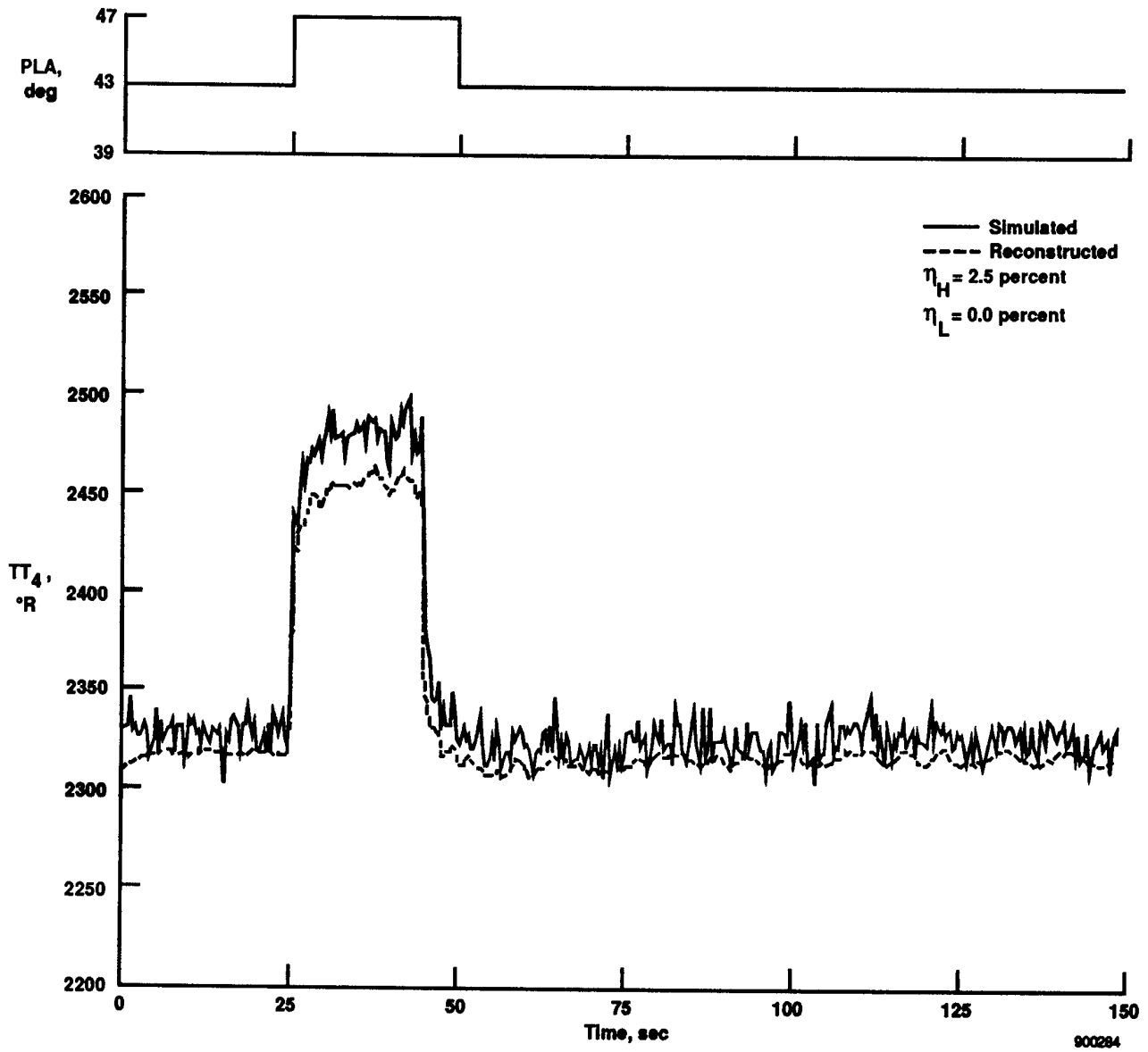
Figure 6. Continued.



900283

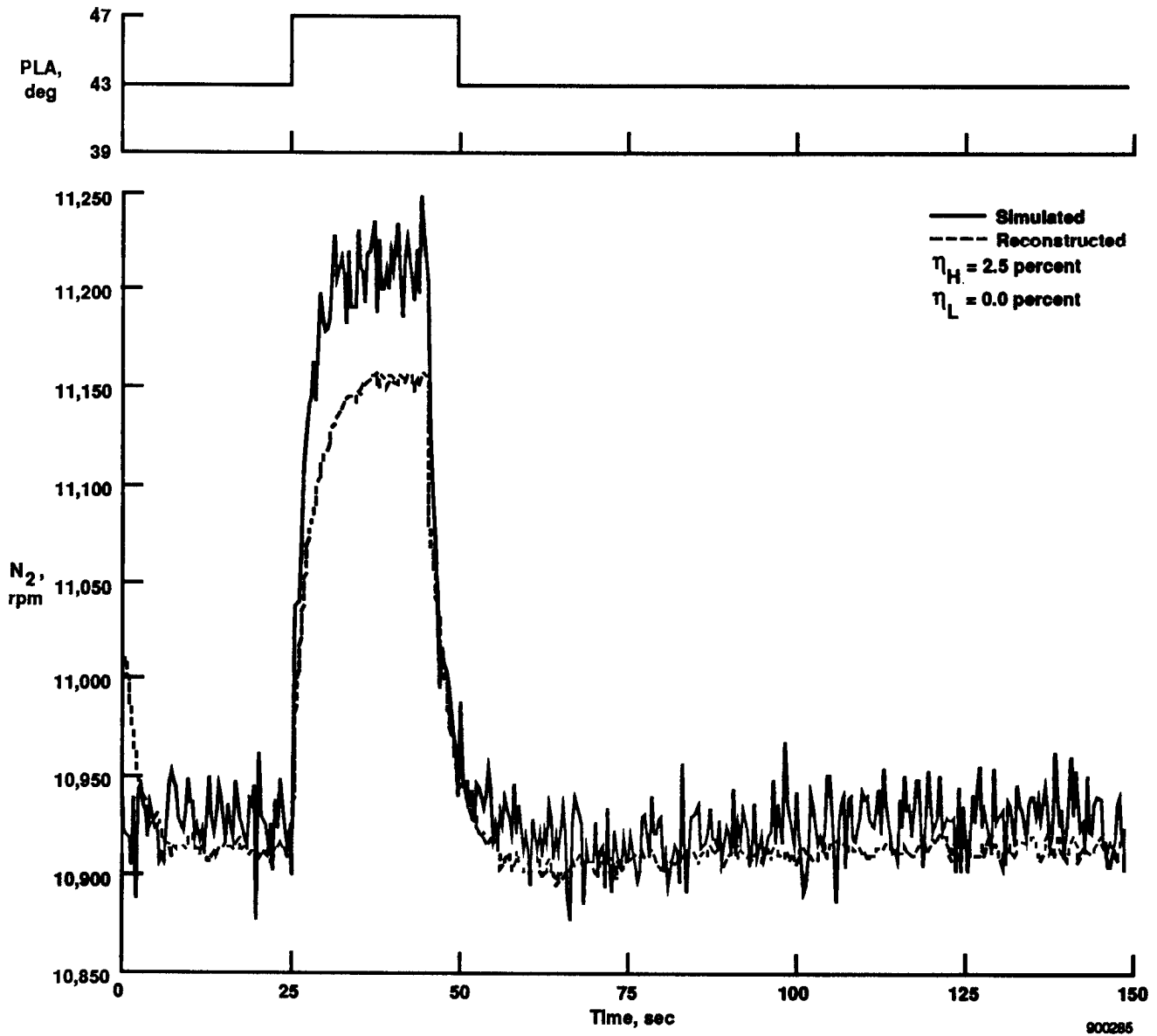
(d) Case 6.

Figure 6. Concluded.



(a) The  $TT_4$  time histories.

Figure 7. Comparison of simulation and reconstructed measurements for case 6.

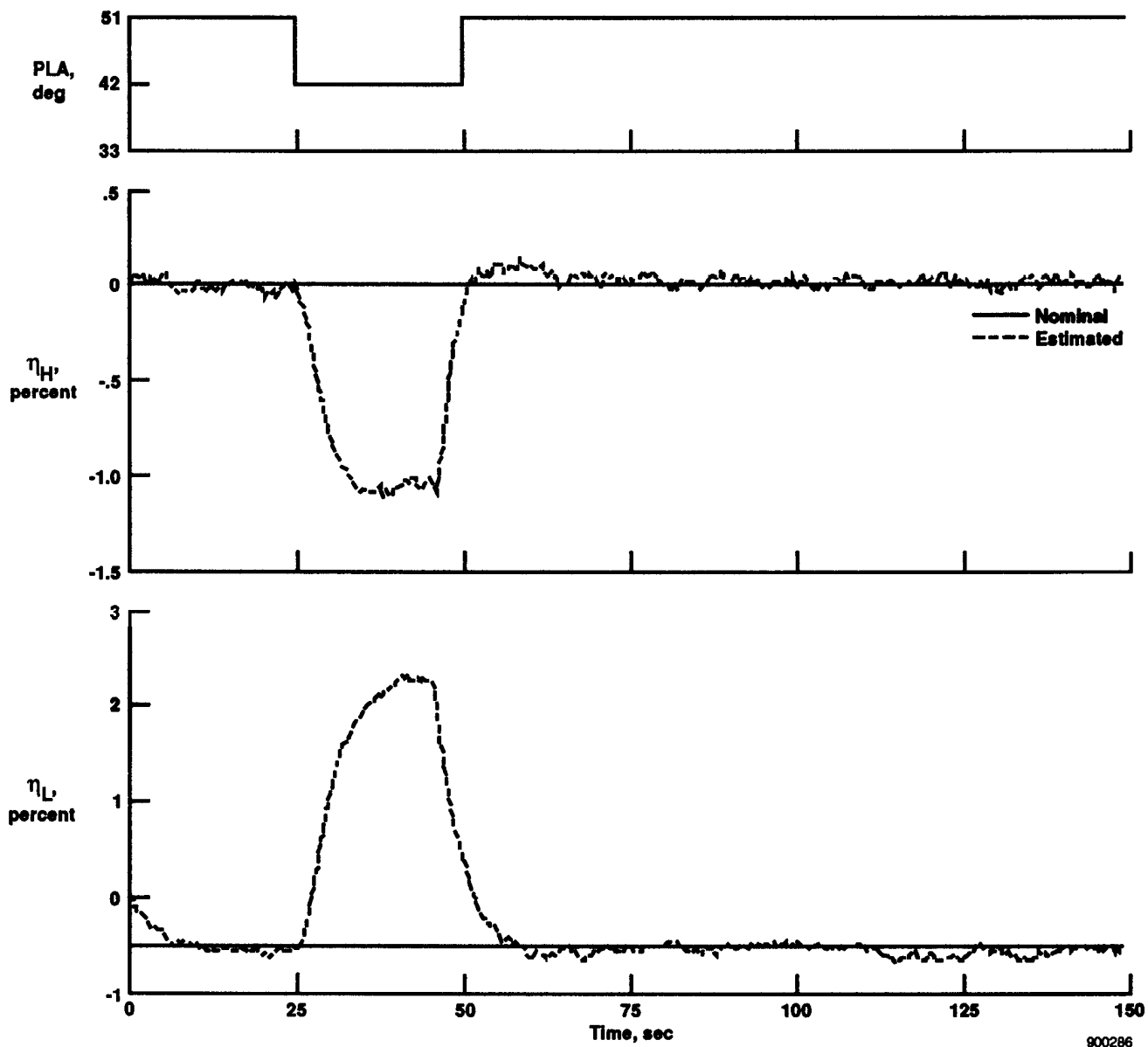


(b) The  $N_2$  time histories.

Figure 7. Concluded.

## Estimation of Low-Pressure Turbine Deterioration

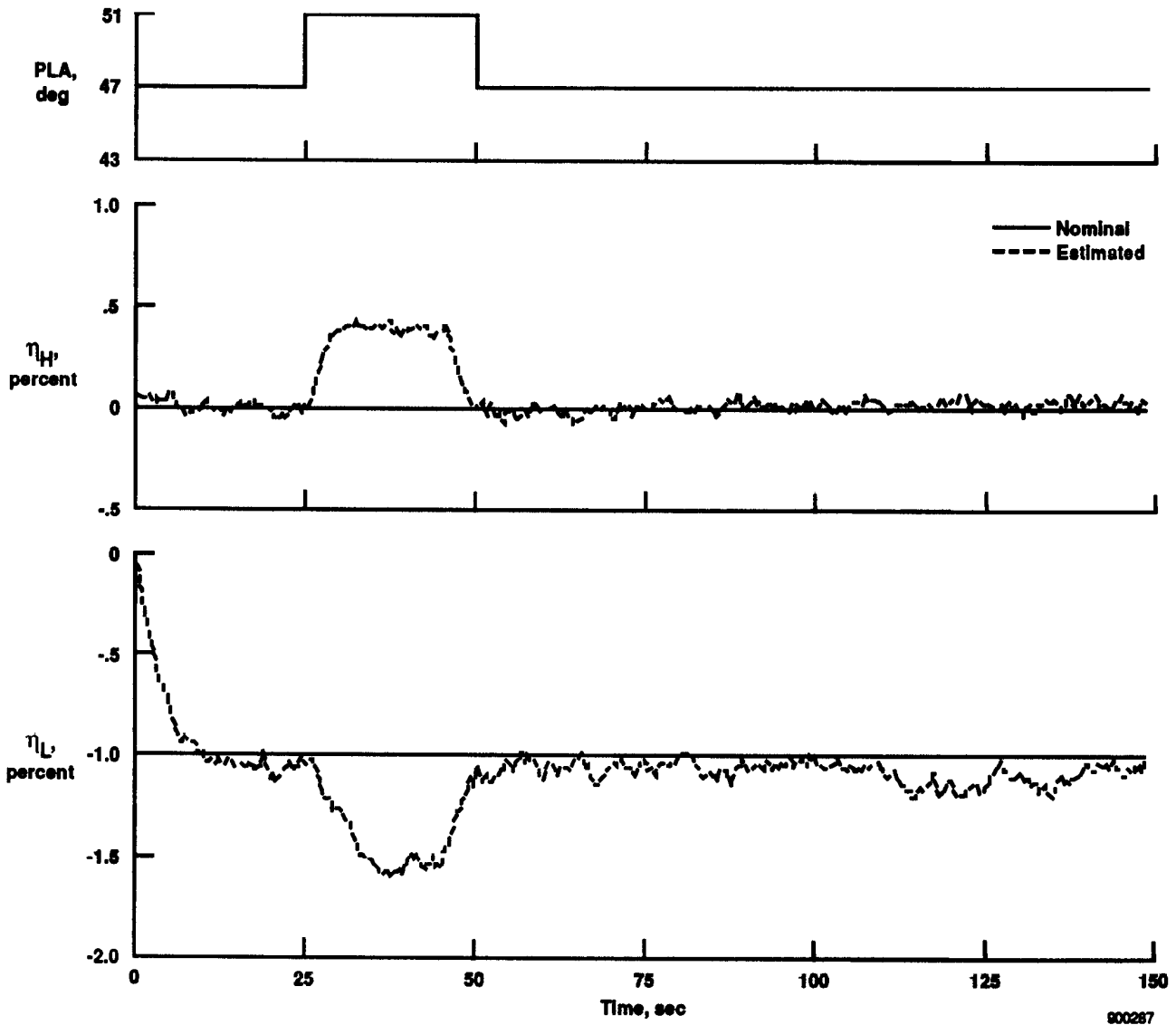
Cases 7–10 represent engine operation with degraded low-pressure turbine efficiency. Figures 8(a)–(d) present the efficiency estimates for cases 7, 8, 9, and 10. The results for cases 7, 8, and 9 are very good. The filter can accommodate –1.0-percent added low-pressure turbine deterioration. The off-design steady-state operation in cases 7 and 9 does not degrade the accuracy of the efficiency estimates. The  $\eta_H$  estimate for case 10 is also well within the desired accuracy of  $\pm 0.25$ -percent efficiency. The  $\eta_L$  estimate for case 10 is poorer than the other cases. The  $\eta_L$  estimate has an absolute error of 0.43-percent efficiency, exceeding the desired accuracy of  $\pm 0.25$ -percent efficiency error. The addition of –2.5-percent low-pressure turbine delta efficiency causes nonlinear effects that exceed the linear range of the model. The poor  $\eta_L$  efficiency estimate for case 10 is reflected in several of the measurement reconstructions. Many of the measured parameters show noticeable increases in difference between the simulation and reconstructed measurement time histories. These parameters are  $TT_4$ ,  $TT_{4.5}$ ,  $TT_6$ , and  $N_2$ . Figures 9(a) and (b) present time history overplots of the simulation and reconstructed measurements for  $TT_{4.5}$  and  $N_2$  for case 10 and are representative of parameters reflecting the poorer efficiency estimates in case 10.



900286

(a) Case 7.

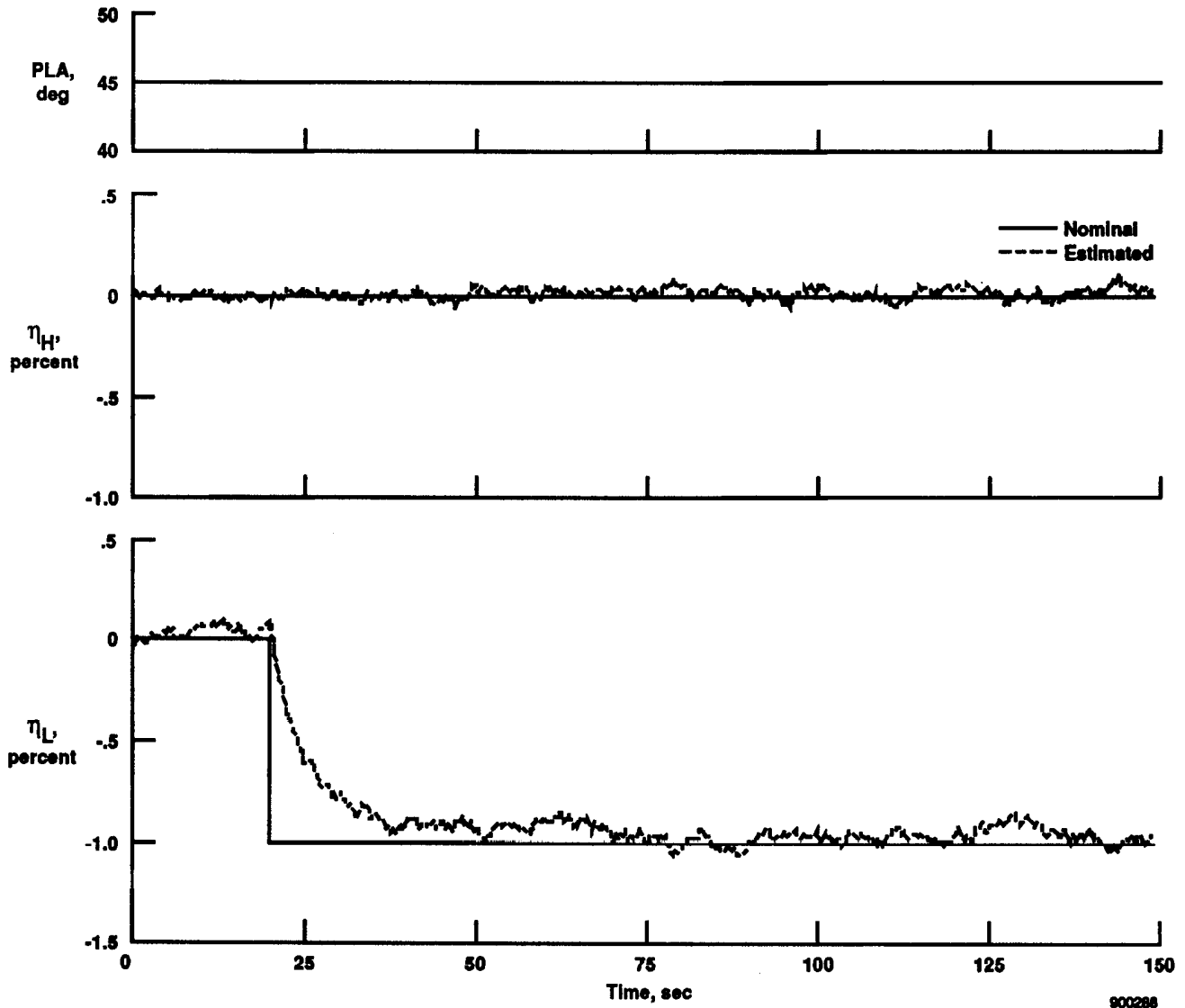
Figure 8. Efficiency estimates.



900287

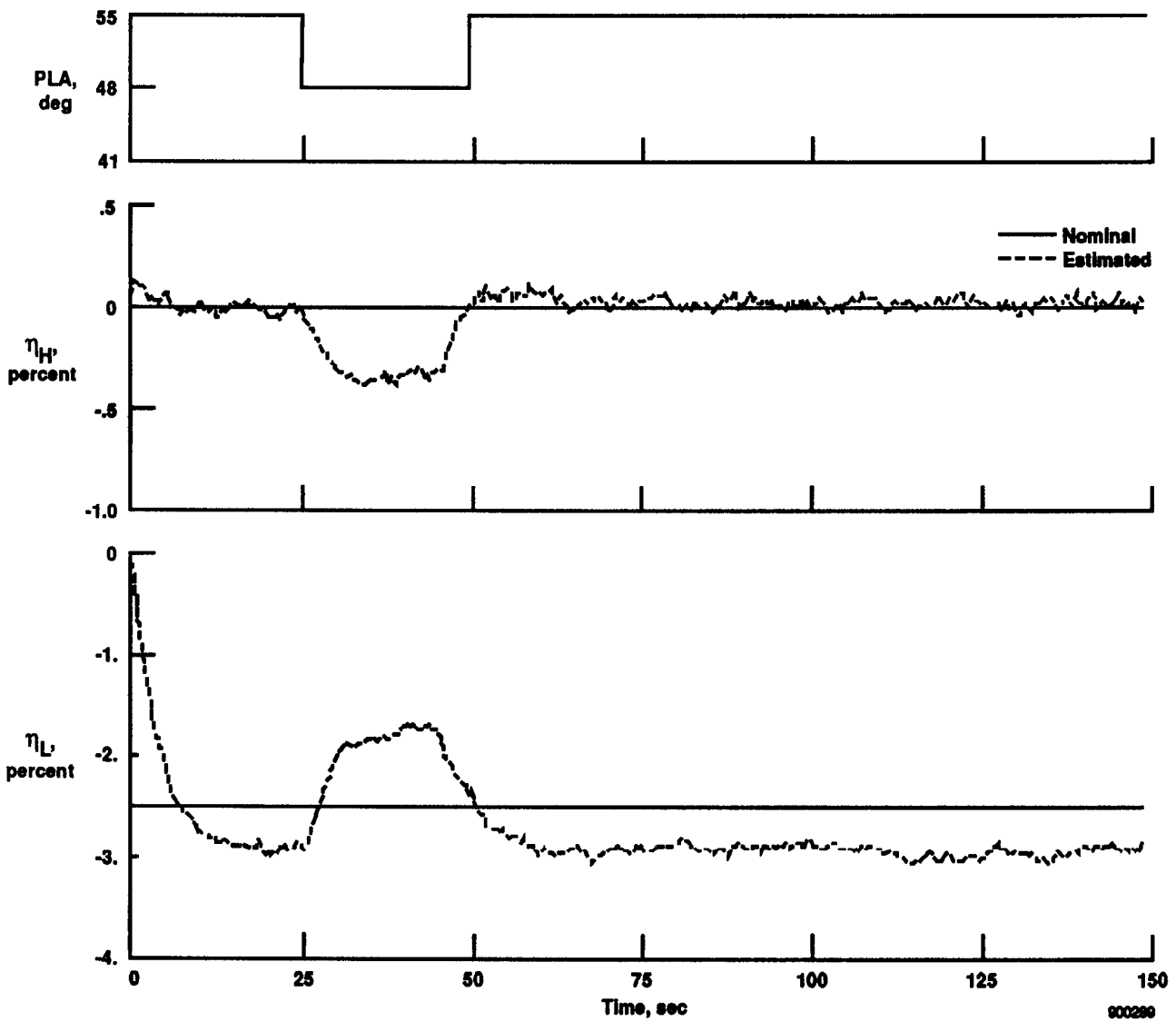
(b) Case 8.

Figure 8. Continued.



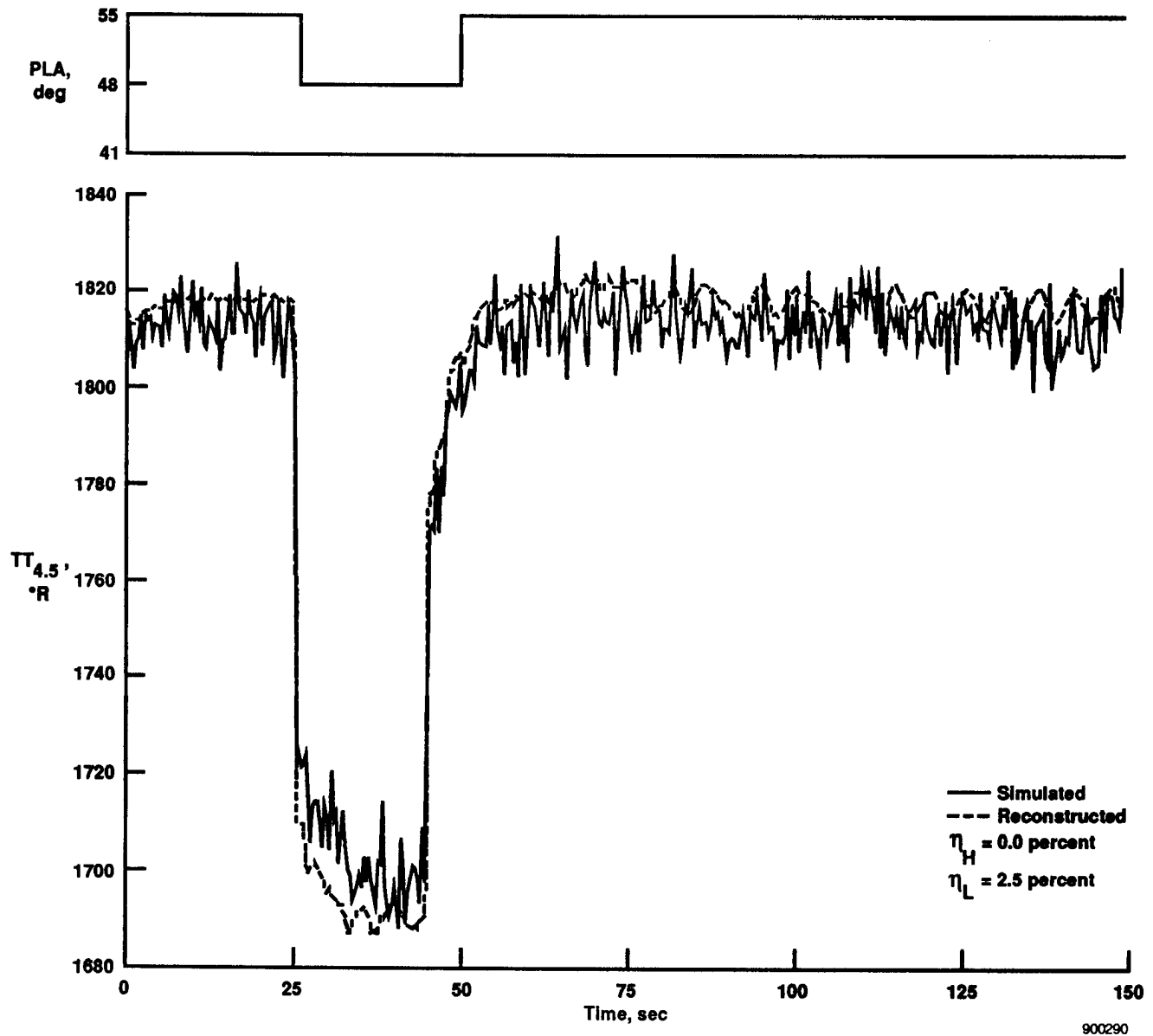
(c) Case 9.

Figure 8. Continued.



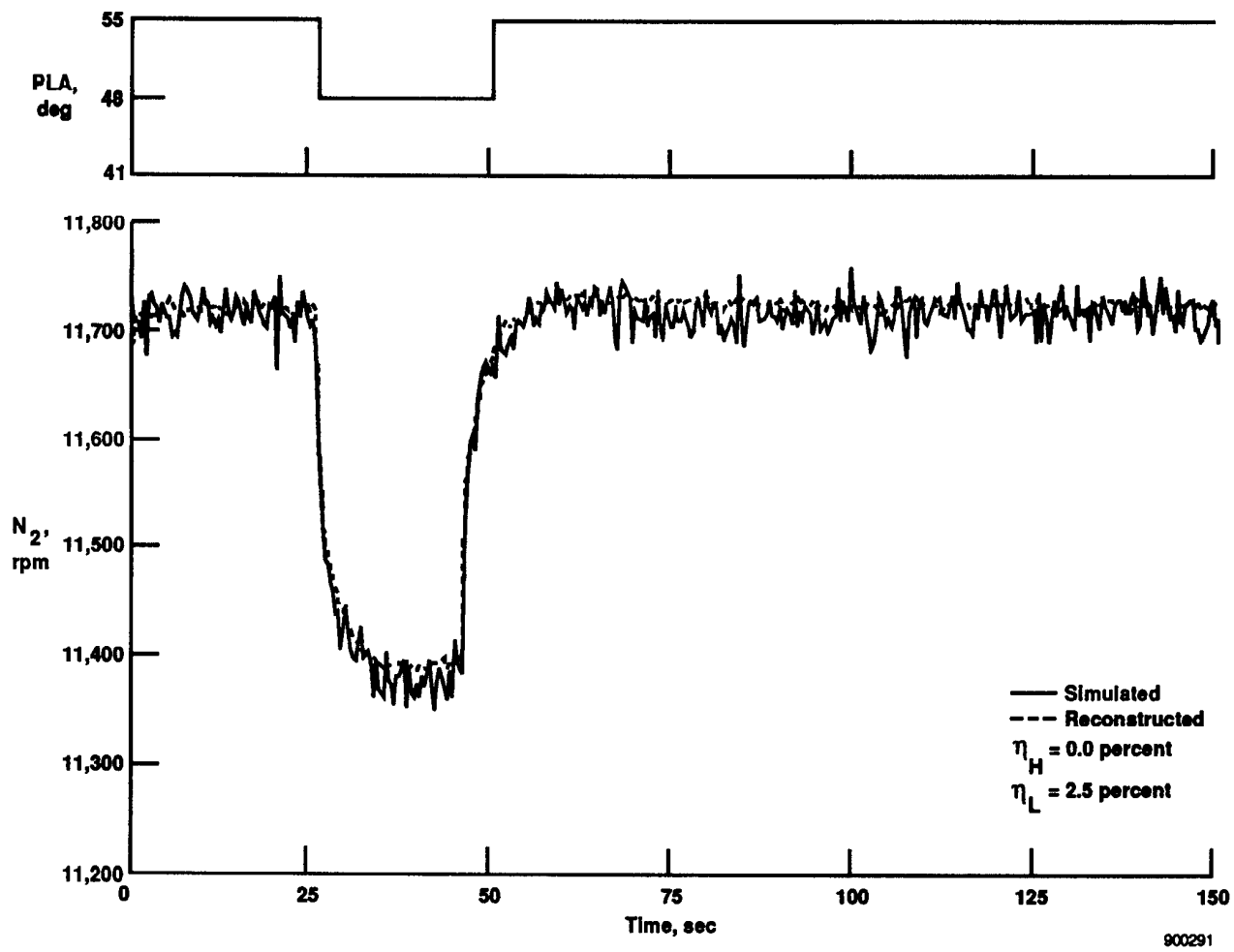
(d) Case 10.

Figure 8. Concluded.



(a) The  $TT_{4.5}$  time histories.

Figure 9. Comparison of simulation and reconstructed measurements for case 10.

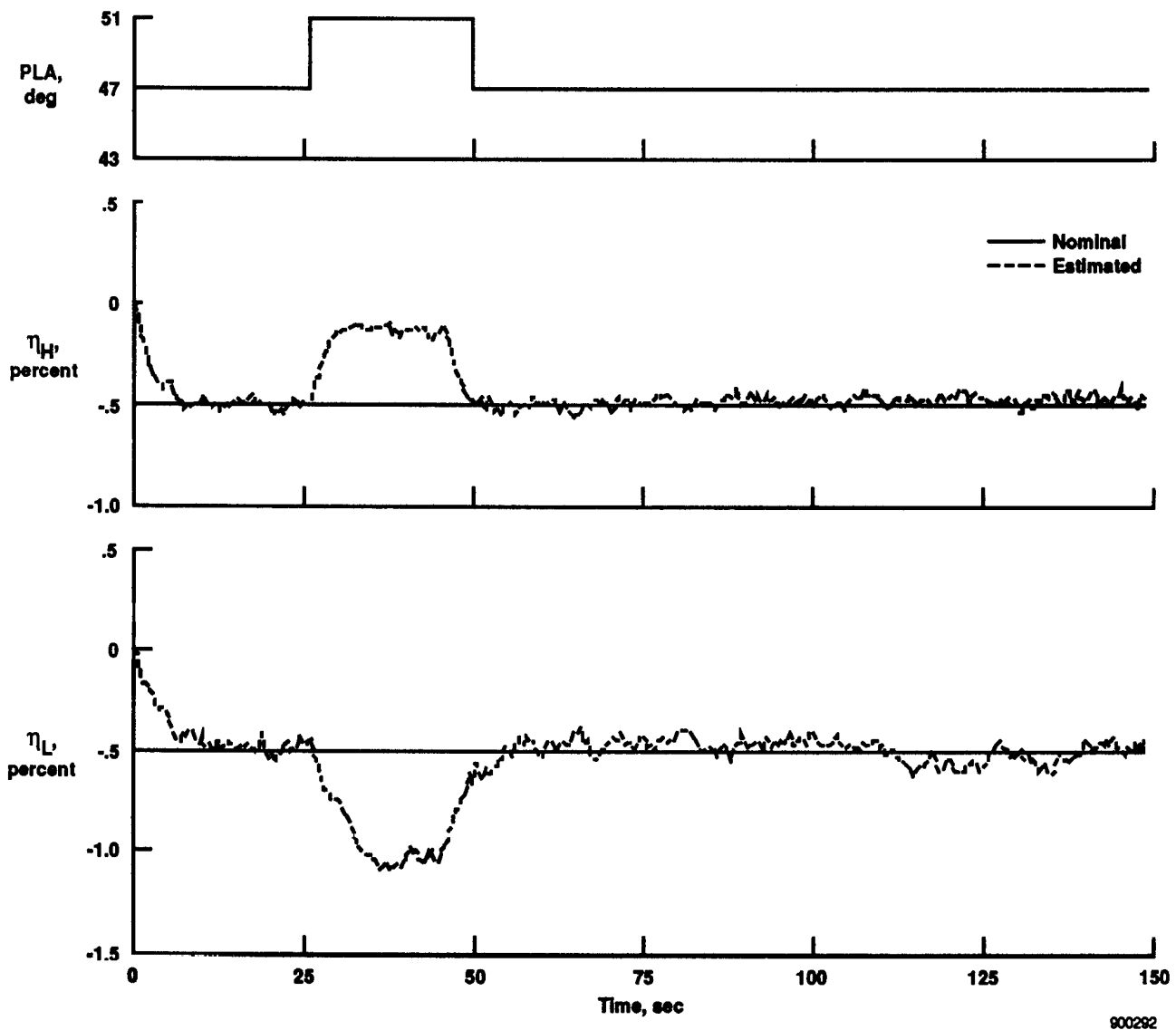


(b) The  $N_2$  time histories.

Figure 9. Concluded.

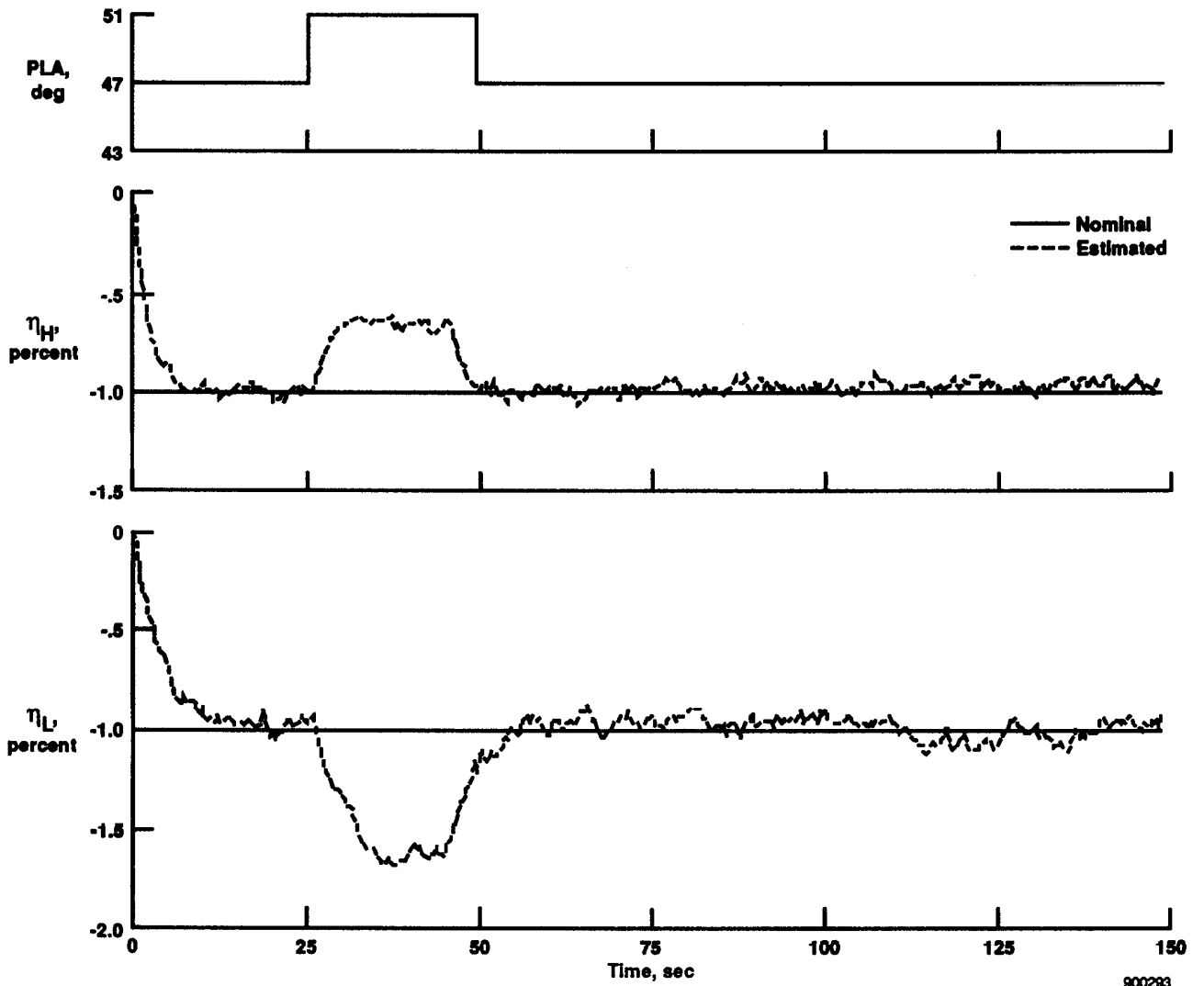
## Estimation With High- and Low-Pressure Turbine Deterioration

Cases 11–14 represent engine operation with degraded high- and low-pressure turbine efficiencies. Figures 10(a)–(d) show the efficiency estimates for these cases. The results for cases 11 and 12 are good. The filter can accommodate  $-1.0$ -percent added high- and low-pressure turbine deterioration at  $47^\circ$  design PLA. The  $\eta_H$  estimate for case 13 is also very good. The  $\eta_L$  estimate for case 13 and both estimates for case 14, although still within the desired accuracy of  $\pm 0.25$ -percent efficiency, are noticeably poorer. The off-design  $45^\circ$  steady-state PLA in case 13 does not degrade the quality of the  $\eta_H$  estimate, but does degrade the  $\eta_L$  estimate. Case 14 has a design steady-state PLA of  $47^\circ$ . The addition of  $-2.5$ -percent high- and low-pressure turbine delta efficiency causes nonlinear effects that exceed the linear range of the model, slightly degrading the quality of the estimates. Figures 11(a) and (b) show representative time history comparisons of the simulation and reconstructed measurements for an engine with high- and low-pressure turbine deterioration. Figure 11(a) is the time history comparison of  $TT_{2.5}$  for case 14. Figure 11(b) is the time history comparison for  $WCFAN$  for case 14.



(a) Case 11.

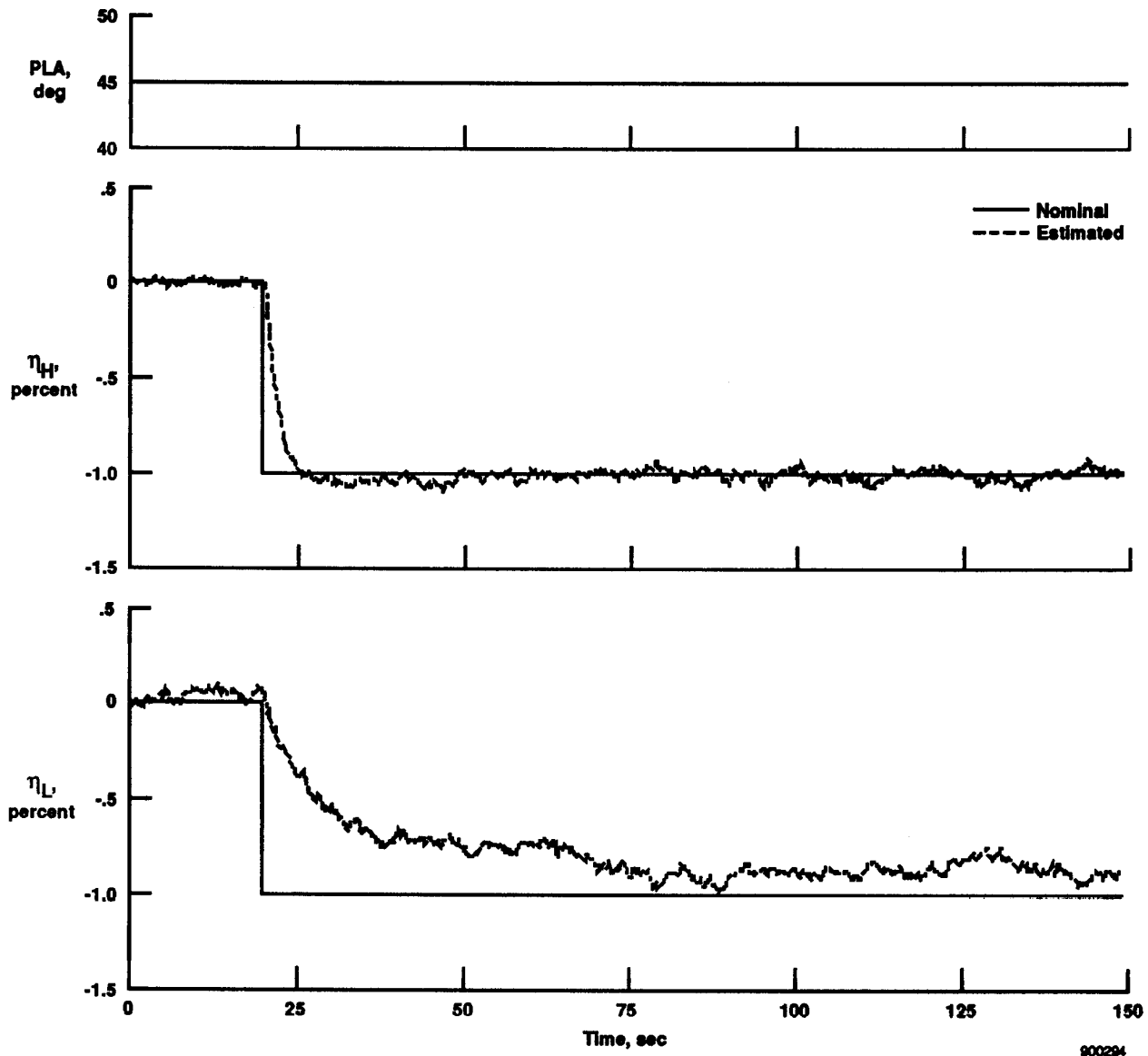
Figure 10. Efficiency estimates.



900293

(b) Case 12.

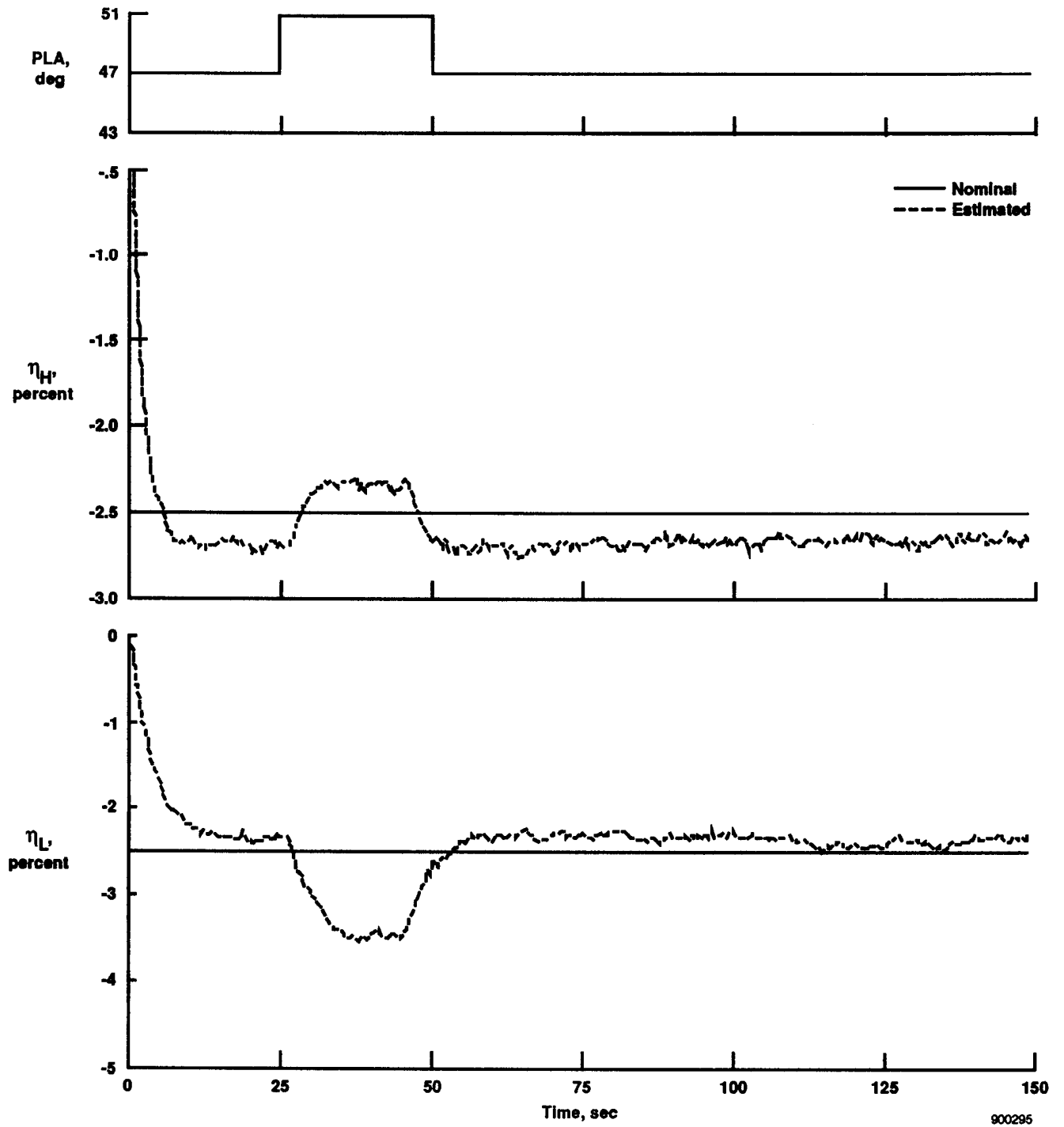
Figure 10. Continued.



900294

(c) Case 13.

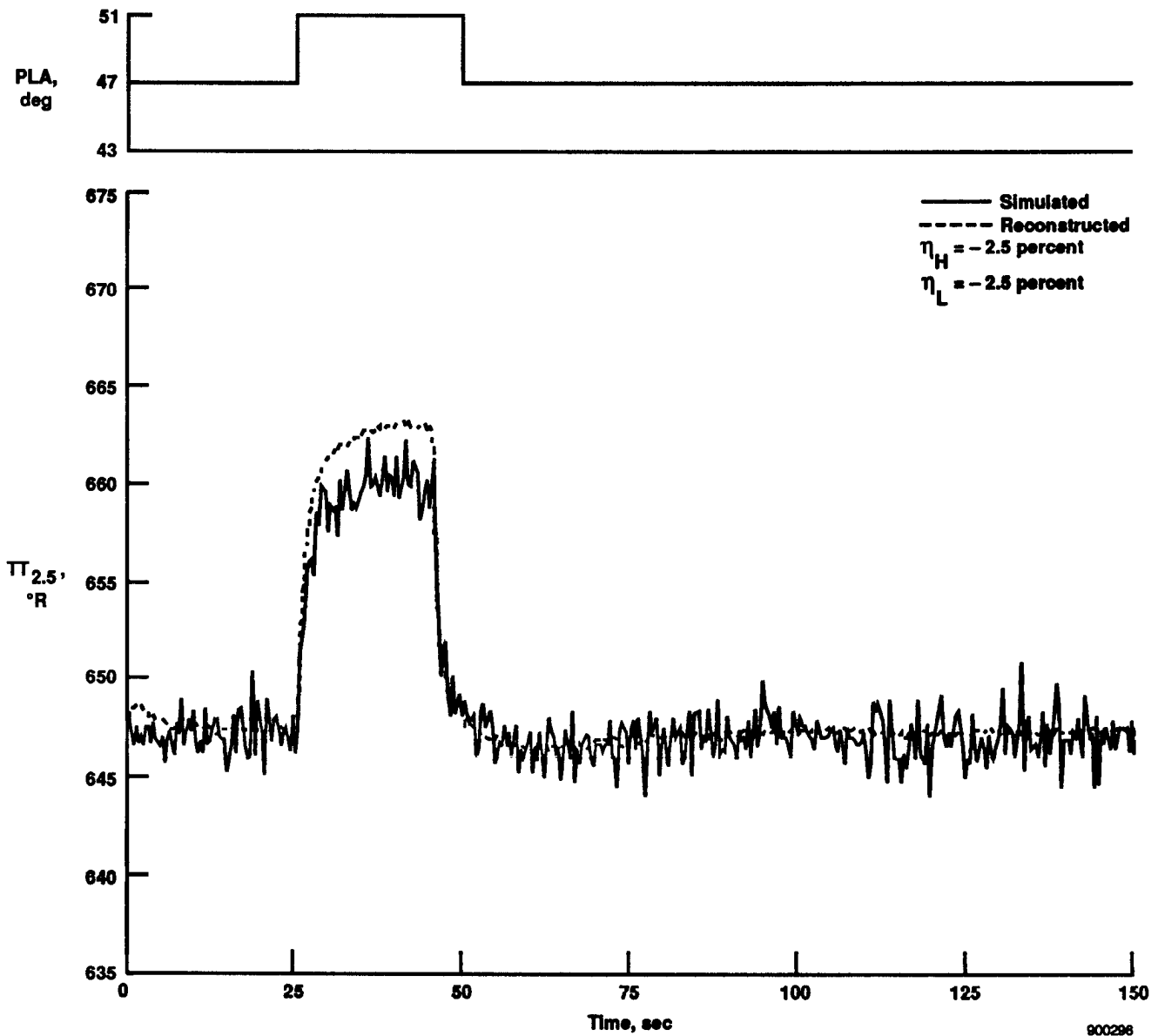
Figure 10. Continued.



(d) Case 14.

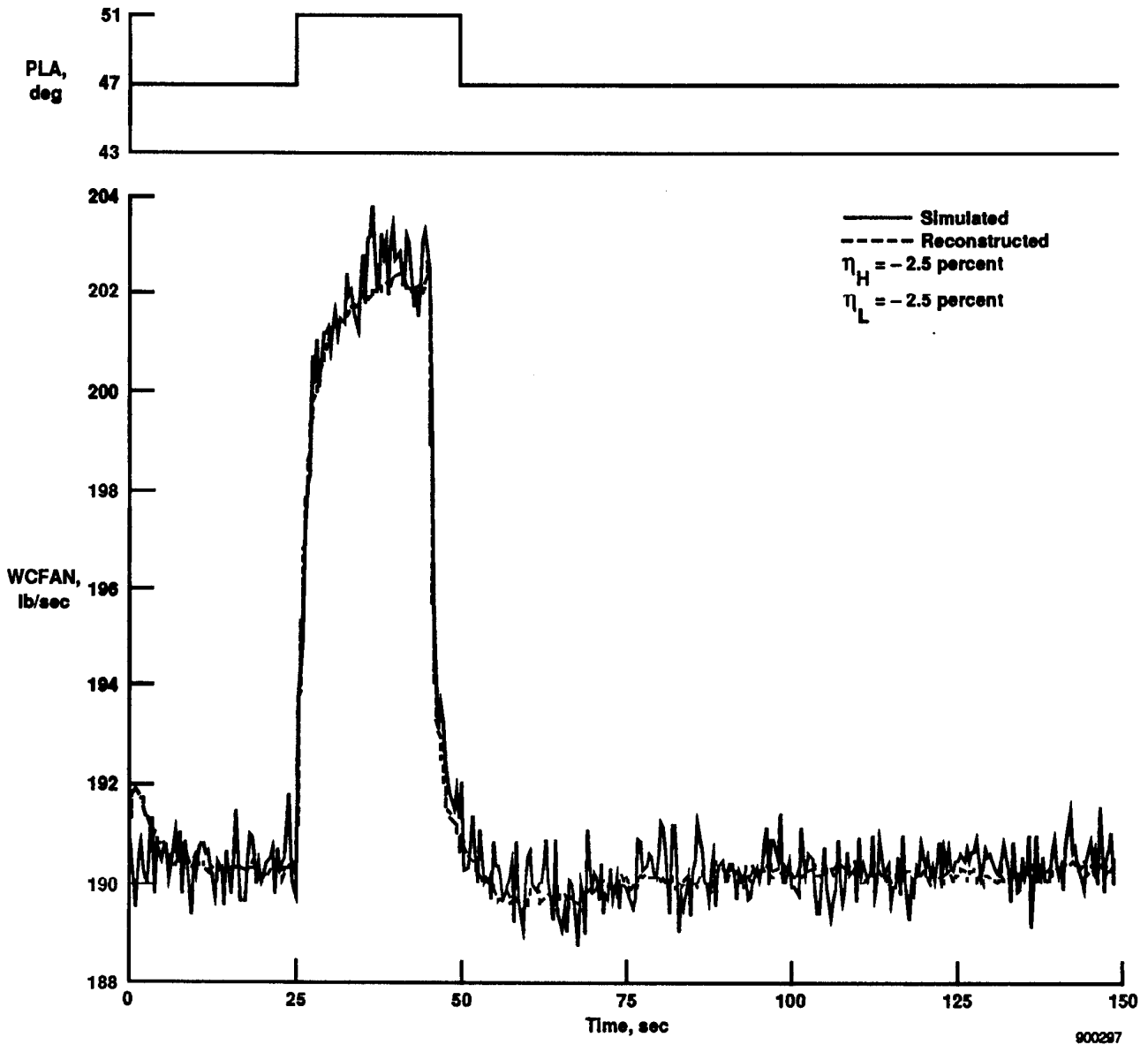
Figure 10. Concluded.

900295



(a) The  $TT_{2.5}$  time histories.

Figure 11. Comparison of simulation and reconstructed measurements for case 14.



(b) The *WCFAN* time histories.

Figure 11. Concluded.

## Evaluation Summary

The Kalman filter design was evaluated with data from a nonlinear engine simulation at Mach 0.90, 30,000-ft altitude, and for trim PLAs in the 43° to 55° range. The filter is able to estimate 2.5-percent high-pressure turbine deterioration within the desired accuracy of  $\pm 0.25$  percent efficiency, independent of the level of low-pressure turbine deterioration. The filter can also estimate  $\eta_L$  within the desired accuracy if the high- and low-pressure turbine deterioration levels are  $\leq 1.0$  percent. During the time history, the estimates account for actual deterioration as well as for deviations from the trim condition. The off-trim operation is reflected primarily in the delta efficiency estimates. When large amounts of deterioration (2.5 percent) are added to either the high- or low-pressure turbine efficiency, the  $\eta_L$  estimate shows errors on the order of  $\pm 0.5$ -percent efficiency. The  $\eta_L$  estimate is highly sensitive to the unmodeled nonlinear effects produced by large delta efficiencies. Cases 6, 10, and 14 show that the filter can identify both estimates with the desired accuracy if large levels of deterioration are added to both the high- and the low-pressure turbine efficiencies. The unmodeled nonlinear effects of the large deterioration in high- and low-pressure turbine delta efficiencies on the  $\eta_L$  estimate are of the same order of magnitude but opposite in sign.

The results of the filter design evaluation indicate that it is able to meet the design criteria for the high-pressure turbine delta efficiency estimate and nearly meets the criteria for the low-pressure turbine delta efficiency estimates.

## CONCLUSIONS

A Kalman filter is designed to estimate the performance deterioration of a simulated F100 engine. The filter design process is straightforward. An important aspect of tuning the Kalman filter is the selection of the state covariance matrix ( $Q_{xx}$ ) and the measurement noise covariance matrix ( $Q_{yy}$ ). The state covariance matrix was selected through an iterative process by comparing the simulation and measurement reconstruction time histories. The process was complicated by the coupling between the fan turbine and low-pressure turbine delta efficiency ( $\eta_L$ ), and between the high-pressure turbine and high-pressure turbine delta efficiency ( $\eta_H$ ). Tuning the  $Q_{xx}$  matrix is the most challenging task in the design process, because of this coupling. The Kalman filter was evaluated using data from a nonlinear engine simulation at Mach 0.90, 30,000-ft altitude, and for trim power lever angles (PLAs) between 43° and 55°. The filter accommodates the desired range of trim PLAs with the desired accuracy. The linear model is valid for engine operation with little or no deterioration. The filter does have some limitations in accommodating the nonlinear effects of high levels of turbine deterioration, particularly for the  $\eta_L$  estimate. The nonlinear effects caused by high levels of deterioration exceed the expected linear range of the model. NASA

*Dryden Flight Research Facility  
National Aeronautics and Space Administration  
Edwards, California, May 9, 1990*

## APPENDIX

### KALMAN FILTER THEORY

The derivation and properties of the Kalman filter are described in references 6–10.

Consider the time-invariant system

$$\delta \dot{x} = A\delta x + B\delta u + w_1 \quad (\text{A-1})$$

$$\delta y = C\delta x + D\delta u + w_2 \quad (\text{A-2})$$

A full-order observer for the system of equations (A-1) and (A-2) can be expressed as

$$\delta \dot{\hat{x}} = A\delta \hat{x} + B\delta u + K [\delta y - (C\delta \hat{x} + D\delta u)] \quad (\text{A-3})$$

where  $K$  is the Kalman filter gain matrix. Rearranging equation (A-3)

$$\delta \dot{\hat{x}} = \begin{bmatrix} A - KC \\ B - KD \quad K \end{bmatrix} \begin{bmatrix} \delta \hat{x} \\ \delta y \end{bmatrix} \quad (\text{A-4})$$

The reconstruction error ( $e$ ) of the observer is defined to be

$$e = x - \hat{x} = \delta x - \delta \hat{x} \quad (\text{A-5})$$

The observer is asymptotically stable, if  $e \rightarrow 0$  as  $t \rightarrow \infty$  for all initial values  $e(t_0)$ .

The Kalman filter is an optimal observer in the sense that the value of the  $K$  matrix minimizes the mean square reconstruction error

$$E\{e^T e\} \quad (\text{A-6})$$

The solution to the optimal observer problem is

$$K = PC^T Q_{yy}^{-1} \quad (\text{A-7})$$

where  $P$  is the solution of the matrix Riccati equation

$$\dot{P} = AP + PA^T + Q_{xx} - PC^T Q_{yy}^{-1} CP \quad (\text{A-8})$$

The solution to the Riccati equation,  $P$ , is the theoretical state estimator error covariance matrix. If a steady-state solution exists, then  $\dot{P} = 0$  for the time invariant case, and hence  $P$ , is the solution to the algebraic Riccati equation

$$0 = AP + PA^T + Q_{xx} - PC^T Q_{yy}^{-1} CP \quad (\text{A-9})$$

The Kalman filter process is shown in figure A-1. The process is implemented as a perturbation formulation. The  $\delta \hat{x}$  is calculated as a linear function of  $\delta \hat{x}$ ,  $\delta u$ ,  $\delta y$ , and  $\delta \hat{y}$

$$\delta \dot{\hat{x}} = \begin{bmatrix} A - KC \\ B - KD \quad K \end{bmatrix} \begin{bmatrix} \delta \hat{x} \\ \delta y \end{bmatrix} \quad (\text{A-10})$$

and is then integrated to obtain  $\delta \hat{x}$ . The  $\delta \hat{y}$  is the measurement perturbation estimate constructed from the state estimate and control perturbations

$$\delta \hat{y} = C\delta \hat{x} + D\delta u \quad (\text{A-11})$$



## REFERENCES

1. Friedland, Bernard, "Treatment of Bias in Recursive Filtering," *IEEE Transactions on Automatic Control*, vol. AC-14, no. 4, 1969.
2. Luppold, R.H., G.W. Gallops, L.J. Kerr, and J.R. Roman, "Estimating In-Flight Engine Performance Variations Using Kalman Filter Concepts," AIAA/ASME/SAE/ASEE 25th Joint Propulsion Conference.
3. Myers, Lawrence P., and Frank W. Burcham, Jr., *Preliminary Flight Test Results of the F100 EMD Engine in an F-15 Airplane*, NASA TM-85902, 1984.
4. *State of the Art Propulsion Program (SOAPP) Simulation*, CCD 1329, Pratt & Whitney, West Palm Beach, Florida.
5. *State Variable Model*, CCD, Pratt & Whitney, West Palm Beach, Florida.
6. Balakrishnan, A.V., *Kalman Filtering Theory*, New York, Springer-Verlag, 1984.
7. Kailath, T., *Lectures on Wiener and Kalman Filtering*, New York, Springer-Verlag, 1981.
8. Kirk, D., *Optimal Control Theory, An Introduction*, Englewood Cliffs, Prentice-Hall, Inc., 1970.
9. Kwakernaak, H., and H. Sivan, *Linear Optimal Control Systems*, New York, Wiley Interscience, 1972.
10. Maybeck, P., *Stochastic Models, Estimation, and Control, Volume 1*, New York, Academic Press, Inc., 1979.
11. *Matrix<sub>x</sub> User's Manual*, Integrated Systems, Inc., 1985.



# Report Documentation Page

1. Report No. NASA TM-104233		2. Government Accession No.		3. Recipient's Catalog No.	
4. Title and Subtitle A Simulation Study of Turbofan Engine Deterioration Estimation Using Kalman Filtering Techniques			5. Report Date June 1991		
			6. Performing Organization Code		
7. Author(s) Heather H. Lambert			8. Performing Organization Report No. H-1616		
			10. Work Unit No. RTOP 533-02-21		
9. Performing Organization Name and Address NASA Dryden Flight Research Facility P.O. Box 273 Edwards, California 93523-0273			11. Contract or Grant No.		
			13. Type of Report and Period Covered Technical Memorandum		
12. Sponsoring Agency Name and Address National Aeronautics and Space Administration Washington, DC 20546-3191			14. Sponsoring Agency Code		
			15. Supplementary Notes		
16. Abstract <p>Current engine control technology is based on fixed control parameter schedules derived for a nominal production engine. Deterioration of the engine components may cause off-nominal engine operation. The result is an unnecessary loss of performance, because the fixed schedules are designed to accommodate a wide range of engine health. These fixed control schedules may not be optimal for a deteriorated engine. This problem may be solved by including a measure of deterioration in determining the control variables. These engine deterioration parameters usually cannot be measured directly but can be estimated.</p> <p>This document presents a Kalman filter design for estimating two performance parameters that account for engine deterioration: high- and low-pressure turbine delta efficiencies. The delta efficiency parameters model variations of the high- and low-pressure turbine efficiencies from nominal values. The filter was evaluated using a nonlinear simulation of the F100 engine model derivative (EMD) engine.</p> <p>This work found that at the model design condition, known high-pressure turbine delta efficiencies of -2.5 percent and low-pressure turbine delta efficiencies of -1.0 percent can be estimated with an accuracy of <math>\pm 0.25</math> percent efficiency with a Kalman filter. If both the high- and low-pressure turbine are deteriorated, then delta efficiencies of -2.5 percent to both turbines can be estimated with the same accuracy.</p>					
17. Key Words (Suggested by Author(s)) Engine deterioration; Engine models; Estimation; Identification; Kalman filter			18. Distribution Statement Unclassified — Unlimited  Subject category 07		
19. Security Classif. (of this report) Unclassified		20. Security Classif. (of this page) Unclassified		21. No. of Pages 47	22. Price A03